1521-0111/86/3/342–357$25.00
MOLECULAR PHARMACOLOGY

http://dx.doi.org/10.1124/mol.114.093286
Mol Pharmacol 86:342–357, September 2014

New Positive Ca^{2+}-Activated K^+ Channel Gating Modulators with Selectivity for $K_{Ca}3.1$ [S]

Nichole Coleman, Brandon M. Brown, Aida Oliván-Viguera, Vikrant Singh, Marilyn M. Olmstead, Marta Sofia Valero, Ralf Köhler, and Heike Wulff

Department of Pharmacology (N.C., B.M.B., V.S., H.W.), School of Medicine, and Department of Chemistry (M.M.O.), University of California, Davis, California; Aragon Institute of Health Sciences, Instituto de Investigación Sanitaria, Fundación Agencia Aragonesa para la Investigación y el Desarrollo, Zaragoza, Spain (A.O.-V., R.K.); and Grupo de Investigación del Medio Ambiente del Centro de Estudios Superiores, Faculty of Health Sciences, Universidad San Jorge, Villanueva de Gállego, Spain (M.S.V.)

Received April 14, 2014; accepted June 23, 2014

ABSTRACT

Small-conductance ($K_{Ca}2$) and intermediate-conductance ($K_{Ca}3.1$) calcium-activated K^+ channels are voltage-independent and share a common calcium/calmodulin-mediated gating mechanism. Existing positive gating modulators like EBIO, NS309, or SKA-31 activate both $K_{Ca}2$ and $K_{Ca}3.1$ channels with similar potency or, as in the case of CyPPA and NS13001, selectively activate $K_{Ca}2.2$ and $K_{Ca}2.3$ channels. We performed a structure-activity relationship (SAR) study with the aim of optimizing the benzothiazole pharmacophore of SKA-31 toward $K_{Ca}3.1$ selectivity. We identified SKA-111 (5-methylnaphtho[1,2-*d*]thiazol-2-amine), which displays 123-fold selectivity for $K_{Ca}3.1$ (EC_{50} 111 ± 27 nM) over $K_{Ca}2.3$ (EC_{50} 13.7 ± 6.9 μM), and SKA-121 (5-methylnaphtho[2,1-*d*]oxazol-2-amine), which displays 41-fold selectivity for $K_{Ca}3.1$ (EC_{50} 109 nM ± 14 nM) over $K_{Ca}2.3$ (EC_{50} 4.4 ± 1.6 μM). Both compounds are 200- to 400-fold selective over representative K_V ($K_V1.3$, $K_V2.1$, $K_V3.1$, and $K_V11.1$), Na_V ($Na_V1.2$, $Na_V1.4$, $Na_V1.5$, and $Na_V1.7$), as well as $Ca_V1.2$ channels. SKA-121 is a typical positive-gating modulator and shifts the calcium-concentration response curve of $K_{Ca}3.1$ to the left. In blood pressure telemetry experiments, SKA-121 (100 mg/kg i.p.) significantly lowered mean arterial blood pressure in normotensive and hypertensive wild-type but not in $KCa3.1^{-/-}$ mice. SKA-111, which was found in pharmacokinetic experiments to have a much longer half-life and to be much more brain penetrant than SKA-121, not only lowered blood pressure but also drastically reduced heart rate, presumably through cardiac and neuronal $K_{Ca}2$ activation when dosed at 100 mg/kg. In conclusion, with SKA-121, we generated a $K_{Ca}3.1$-specific positive gating modulator suitable for further exploring the therapeutical potential of $K_{Ca}3.1$ activation.

Introduction

The human genome contains four voltage-independent Ca^{2+}-activated K^+ channels: the three small-conductance $K_{Ca}2$ channels: $K_{Ca}2.1$ (= KCNN1, SK1), $K_{Ca}2.2$ (= KCNN2, SK2), and $K_{Ca}2.3$ (= KCNN3, SK3), as well as the intermediate-conductance $K_{Ca}3.1$ (= KCNN4, IK1, SK4) (Kohler et al., 1996; Joiner et al., 1997; Wei et al., 2005). Their lack of voltage dependence enables these channels to remain open at negative membrane potentials and to hyperpolarize the membrane toward values near the K^+ equilibrium potential of −89 mV. $K_{Ca}3.1$ and $K_{Ca}2$ channels are accordingly expressed in cells that need to be able to hyperpolarize to regulate Ca^{2+} influx through inward rectifier Ca^{2+} channels, pass on hyperpolarization

This work was supported by the CounterACT Program, National Institutes of Health (NIH) Office of the Director [Grant U54NS079202] and National Institute of Neurological Disorders and Stroke [R21NS072585], the Deutsche Forschungsgemeinschaft [Grant KO1899/11-1], the Danish Hjerteforening, and the Fondo de Investigación Sanitaria [Red HERACLES RD12/0042/0014]. N.C. was supported by an NIH National Heart, Lung and Blood Institute T32 Training Program in Basic and Translational Cardiovascular Science [Grant T32HL086350]. B.M.B. was supported by an NIH National Institute of General Medical Sciences–funded Pharmacology Training Program [Grant T32GM099608].

N.C. and B.M.B. contributed equally to this work. R.K. and H.W. are co-senior authors.

The work forms part of the Ph.D. thesis of Nichole Coleman in fulfillment of the degree requirements of the University of California, Davis.

dx.doi.org/10.1124/mol.114.093286.

[S] This article has supplemental material available at molpharm.aspetjournals.org.

ABBREVIATIONS: BK, bradykinin; CaM, calmodulin; CamBD, calmodulin binding domain; CAS, Chemical Abstracts Service; CM-TMF, *N*-{7-[1-(4-chloro-2-methylphenoxy)ethyl]-[1,2,4]triazolo[1,5-*a*]pyrimidin-2-yl}-*N*'-methoxy-formamidine; CyPPA, cyclohexyl-[2-(3,5-dimethyl-pyrazole-1-yl-)6-methyl-pyrimidin-4-yl]-amine; DMSO, dimethylsulfoxide; EBIO, 1-ethylbenzimidazolin-2-one; EDH, endothelium-derived hyperpolarization; HEK, human embryonic kidney; HR, heart rate; HRMS, high-resolution mass spectrometry; K_{Ca}, Ca^{2+}-activated K^+ channel; $K_{Ca}3.1$, intermediate-conductance Ca^{2+}-activated K^+ channel; K_V, voltage-gated K^+ channel; LC, liquid chromatography; MAP, mean arterial blood pressure; m.p., melting point; MS, mass spectrometry; NMR, nuclear magnetic resonance; NS309, 6,7-dichloro-1*H*-indole-2,3-dione 3 oxime; PCA, porcine coronary arteries; SK, small-conductance K_{Ca} channel; SKA-31, naphtho[1,2-*d*]thiazol-2-ylamine; SKA-111, 5-methylnaphtho[1,2-*d*]thiazol-2-amine; SKA-121, 5-methylnaphtho[2,1-*d*]oxazol-2-amine; TRAM-34, 1-[(2-chlorophenyl)diphenylmethyl]-1*H*-pyrazole; UCL1684, 6,10-diaza-3(1,3)8,(1,4)-dibenzena-1,5(1,4)-diquinolinacyclodecaphane; U46619, (*Z*)-7-[(1*S*,4*R*,5*R*,6*S*)-5-[(*E*,3*S*)-3-hydroxyoct-1-enyl]-3-oxabicyclo[2.2.1]heptan-6-yl]hept-5-enoic acid; UPLC, ultraperformance liquid chromatography.

through gap junctions, or regulate firing frequency by preventing an untimely or premature action potential initiation (Adelman et al., 2012; Wulff and Köhler, 2013). Pharmacologic activation of K_{Ca} channels has therefore been suggested for the treatment of various diseases. Whereas $K_{Ca}2$ activators can potentially reduce neuronal excitability in central nervous system disorders like epilepsy and ataxia, $K_{Ca}3.1$ activators could be useful as endothelial targeted antihypertensives and to enhance fluid secretion in the airways in cystic fibrosis (Wulff and Zhorov, 2008; Balut et al., 2012; Wulff and Köhler, 2013).

All four $K_{Ca}2/3$ channels are voltage-independent and share a Ca^{2+}/calmodulin-mediated gating mechanism (Xia et al., 1998; Fanger et al., 1999). Calmodulin (CaM), which can be regarded as a β-subunit for these channels, is constitutively bound to a CaM-binding domain (CaMBD) in the intracellular C-terminus. On Ca^{2+} binding to CaM, the channels activate in a highly coordinated fashion with an extremely steep Hill equation and EC_{50} values in the range of 250–900 nM (Wei et al., 2005). $K_{Ca}2/3$ activators modulate this gating process and have therefore been termed *positive gating modulators*. The oldest positive modulator of $K_{Ca}2/3$ channels is the benzimidazolone EBIO (Devor et al., 1996), which activates $K_{Ca}3.1$ with an EC_{50} of ~30 μM and all three $K_{Ca}2$ channels with EC_{50}s around 300 μM (Wulff and Köhler, 2013). Two structurally similar, but more potent molecules, are the oxime NS309 (Strobaek et al., 2004) and the benzothiazole SKA-31 (Sankaranarayanan et al., 2009). Whereas NS309 is exquisitely potent (EC_{50} for $K_{Ca}3.1$ ~20 nM; EC_{50} for $K_{Ca}2$ channels ~600 nM), it unfortunately has an extremely short in vivo half-life and inhibits $K_V11.1$ (hERG) at a concentration of 1 μM (Strobaek et al., 2004). SKA-31 is 10 times less potent than NS309 but has become a relatively widely used in vivo tool compound to activate both $K_{Ca}3.1$ and/or $K_{Ca}2$ channels because of its long half-life of 12 hours in rats (Sankaranarayanan et al., 2009). In contrast to these benzimidazole/benzothiazole-type K_{Ca} activators, all of which show only a modest 5- to 10-fold selectivity for $K_{Ca}3.1$ and do not distinguish at all between the three $K_{Ca}2$ channels, CyPPA, and its derivative NS13001, have quite different selectivity profiles. Both compounds activate $K_{Ca}2.3$ and $K_{Ca}2.2$ but are completely inactive on $K_{Ca}2.1$ and $K_{Ca}3.1$ (Hougaard et al., 2007; Kasumu et al., 2012). GW542573X and (-)-CM-TMPF, in contrast, are selective for $K_{Ca}2.1$ (Hougaard et al., 2009, 2012). So while there are some compounds that allow for the selective pharmacologic activation of $K_{Ca}2$ channels, there currently is no selective $K_{Ca}3.1$ activator.

We previously used riluzole, a drug for the treatment of amyotrophic lateral sclerosis, as a template for the design of SKA-31. Riluzole is a "dirty" compound that exerts multiple pharmacological activities, the most prominent of which are inhibition of voltage-gated sodium (Na_V) channels at concentrations of 1–50 μM (Debono et al., 1993; Duprat et al., 2000) and activation of $K_{Ca}2/3$ channels with EC_{50}s of 10–20 μM (Grunnet et al., 2001). Through directed derivatization of riluzole, we managed to significantly reduce Na_V channel blocking effects and increase activity on $K_{Ca}2/3$ channels. Whereas SKA-31 affects Na_V channels only at concentrations of 25 μM or higher, it activates $K_{Ca}2.3$ with an EC_{50} of 3 μM and $K_{Ca}3.1$ with an EC_{50} of 260 nM. Since both $K_{Ca}3.1$ and $K_{Ca}2.3$ are expressed in vascular endothelium and have been shown to be involved in the so-called endothelium-derived hyperpolarization (EDH) response (Grgic et al., 2009; Dalsgaard et al., 2010; Edwards et al., 2010; Köhler et al., 2010), SKA-31 was used as a pharmacologic tool to explore the role of K_{Ca} channels in blood pressure regulation. While mice deficient in $K_{Ca}3.1$ and/or $K_{Ca}2.3$ exhibit impaired EDH responses and an increased mean arterial blood pressure (MAP) (Brahler et al., 2009), pharmacologic K_{Ca} channel activation with SKA-31 lowered blood pressure in both mice and dogs (Sankaranarayanan et al., 2009; Damkjaer et al., 2012; Radtke et al., 2013). In dogs, i.v. injection of 2 mg/kg SKA-31 produced an immediate and strong (−30 mmHg) but short-lived reduction in blood pressure (Damkjaer et al., 2012). In mice, SKA-31 doses of 10–30 mg/kg have been reported to lower blood pressure more prolonged (~30 mmHg) for 60–90 minutes) (Sankaranarayanan et al., 2009; Köhler, 2012). Significant blood pressure–lowering effects with SKA-31 doses of 30 mg/kg have been further observed in models of hypertension like angiotensin II–infused (Sankaranarayanan et al., 2009) and connexin 40–deficient mice (Radtke et al., 2013), which exhibit severe chronic renin-dependent hypertension. However, the responses typically lasted only about 1 hour. Higher doses of SKA-31 (100 mg/kg) induced a stronger and longer-lasting response, accompanied by significant bradycardia. This reduction in heart rate (HR) was probably due to a centrally mediated decrease in sympathetic drive through activation of neuronal $K_{Ca}2$ channels by the brain penetrant SKA-31, as well as possible direct effects on $K_{Ca}2$ channels in cardiac pacemaker tissue (Radtke et al., 2013). Another side effect that might prohibit the use of $K_{Ca}2$ activators as antihypertensives is a possible impairment of learning and memory because of the role neuronal $K_{Ca}2$ channels play in in synaptic plasticity and long-term potentiation (Blank et al., 2003; Adelman et al., 2012). To avoid these $K_{Ca}2$ channel–mediated side effects, it therefore seems highly desirable to identify selective $K_{Ca}3.1$ activators that could be used as pharmacological tools to further dissect the in vivo role of $K_{Ca}3.1$ in blood pressure control and to help determine whether $K_{Ca}3.1$ activators could eventually be developed into a new class of endothelial-targeted antihypertensives. We therefore here explored whether we could further modify the benzothiazole SKA-31 and develop a $K_{Ca}3.1$-selective small-molecule activator. SKA-121, a compound generated through an isosteric replacement approach, activates $K_{Ca}3.1$ with an EC_{50} of 111 nM, exhibits 40- to 80-fold selectivity over the three $K_{Ca}2$ channels and lowers blood pressure in mice as determined by telemetry without exerting $K_{Ca}2$ channel–mediated effects on HR. We propose SKA-121 as a new $K_{Ca}3.1$ selective pharmacological tool compound despite its relatively short half-life in mice.

Materials and Methods

Commercially Available Compounds

2-Amino-4-(1-naphthyl)thiazole (SKA-75, CAS no. 56503-96-9), 2-amino-4-(2-naphthyl)thiazole (SKA-76), Chemical Abstracts Service (CAS) no. 21331-43-1), 2,3,3-trimethyl-3*H*-benzo[*g*]indole (SKA-92, CAS no. 74470-85-2), 2-methylnaphtho[2,3-*d*]oxazole (SKA-104, CAS no. 20686-66-2), and 2-methylnaphtho[2,1-*d*]oxazole (SKA-103, CAS no. 85-15-4) were purchased from Alfa Aesar (Pelham, NH); 2-methylnaphtho[1,2-*d*]thiazole (SKA-74, 2682-45-3) was purchased from Sigma (St. Louis, MO).

Chemical Synthesis

Compounds that were not commercially available were synthesized in our laboratory by the general methods described below. Compounds reported previously were characterized by melting point, proton nuclear magnetic resonance (^{1}H NMR) and 13 carbon (13C) NMR to confirm their chemical identity. New chemical entities were additionally characterized by high-resolution mass spectrometry (HRMS) and a fully interpreted ^{13}C NMR.

General Method I. Preparation of Thiazoles. Thiourea (17 mmol) was added to a solution of substituted ketones (6 mmol) in 30 ml of absolute ethanol. The mixture was refluxed for 8 hours, which resulted in 2-aminothiazole hydrobromide salts. The 2-aminothiazole was obtained by treating the hydrobromide salt with 2M NaOH (5 ml) and extracting with ethyl acetate. The crude residue was concentrated, reconstituted in a methanol-water mixture (99:1), treated with charcoal, and recrystallized.

General Method II. Alternative Preparation of Benzothiazoles. Thiourea (17 mmol) was added to a solution of substituted ketones (6 mmol) in 30 ml of absolute ethanol. The mixture was refluxed for 8 hours, which resulted in 2-aminothiazole hydrobromide salts. The free 2-aminothiazole was obtained by treating the hydrobromide salt with 2 M NaOH (5 ml) and extracting with ethyl acetate. The crude residue was concentrated, reconstituted in a methanol-water mixture (99:1), treated with charcoal, and recrystallized. The resulting 2-aminothiazole, 2-iodoxybenzoic acid and tetrabutylammonium tribromide were combined in ethyl acetate and stirred at room temperature (RT) for 10 hours. The reaction mixture was filtered through a pad of Celite, and the filtrate was diluted with saturated $Na_2S_2O_3$ and extracted with ethyl acetate. The combined organic layers were dried with anhydrous sodium sulfate (anhydrous Na_2SO_4), concentrated, and then purified via flash chromatography (cyclohexane-EtOAc, 1:1).

General Method III. Preparation of Benzothiazoles. Benzoyl chloride was added drop wise to a stirred solution of NH_4SCN in acetone and stirred at 50°C for 2 hours. Next, a solution of substituted naphthylamines in acetone was added drop wise, and the mixture was stirred at 50°C for 24 hours. The reaction mixture was diluted with water; the precipitated crystals collected by filtration and washed with water. The crystals were then suspended in 2M NaOH (50 ml), refluxed for 1 hour, and poured into cold water and filtered. The crude crystals of the resulting thiourea were dissolved in acetic acid, to which benzyl trimethylammonium tribromide was added and allowed to react overnight. Ethyl ether (Et_2O) was added and the precipitate of the resulting product-HBr salt was collected by filtration and washed with Et_2O. The salt was then treated with 1M NaOH to liberate the free base, which was recrystallized in methanol.

General Method IV. Preparation of 2-Aminonaphthooxazoles. To procure the intermediate 2-hydroxy-naphthalenones, substituted ketones (1 g, 6.2 mmol) were added to a stirred mix of water (25 ml), acetonitrile (25 ml) trifluoroactic acid (6 ml, 7 mmol), iodobenzene (0.7 ml, 6 mmol), and oxone (11 g, 37 mmol). The resulting solution was refluxed for 1 hour, and the progress of the reaction was monitored by thin layer chromatography (TLC). The reaction was then allowed to cool to RT and filtered. The mixture was extracted with ethyl acetate (3 × 30 ml) and lastly neutralized with saturated $NaHCO_3$ (3 × 30 ml). The combined organic phase was washed with brine (30 ml), dried with anhydrous Na_2SO_4, filtered, and concentrated. The residue was purified by flash chromatography over silica gel (cyclohexane-EtOAc, 3:1) to give substituted 2-hydroxy-naphthalenones (R_f = 0.20). The preparation of 2-aminonaphthooxazole began by adding cyanamide (2 mmol) to a stirred solution of substituted 2-hydroxy-naphthalenone (1.5 mmol), water (20 ml), and acetonitrile (10 ml). The resulting mixture was refluxed for 15 hours, and progression of the reaction was monitored by TLC. The reaction was allowed to cool to RT. The mixture was extracted with ethyl acetate (3 × 30 ml) to give a mixture of isomers. The combined organic phase was washed with brine (30 ml), dried with anhydrous Na_2SO_4, filtered, and concentrated. The isomers were purified and separated by flash chromatography over silica gel (cyclohexane-EtOAc, 1:1).

8*H*-Indeno[1,2-*d*]thiazol-2-amine (SKA-69). SKA-69 was prepared from 1-indanone (1 g, 4.7 mmol) according to general method I. The product was isolated as brown crystals (563 mg, 63%); melting point (m.p.) = 212°C (CAS no. 85787-95-7). ^{1}H NMR [500 MHz, dimethylsulfoxide (DMSO)-d_6, δ]: 7.45 (doublet (d), J = 7.4 Hz, 1H, 4-H), 7.37 (d, J = 7.4 Hz, 1H, 7-H), 7.28 (t, J = 7.4 Hz, 1H, 5-H), 7.17–7.11 (m, 3H, 6-H, and NH_2), 3.68 (s, 2H, CH_2). ^{13}C NMR (125 MHz: DMSO-d_6, δ):173.74, 146.09, 138.04, 128.58, 126.68, 126.60, 125.47, 118.2, and 32.85.

4,5-Dihydronaphtho[1,2-*d*]thiazol-2-amine (SKA-70). SKA-70 was prepared from 1-tetralone (1 g, 6.84 mmol) according to general method I. The product was isolated as white crystals (906 mg, 64%); m.p. = 135°C (CAS no. 34176-49-3). ^{1}H NMR (500 MHz, DMSO-d_6, δ): 7.52 (d, J = 7.3 Hz, 1H, 9-H), 7.23−7.14 (m, 2H, 7-H and 6-H), 7.10 (t, J = 7.3 Hz, 1H, 8-H), 6.93 (s, 2H, NH_2), 2.93 (t, J = 7.8 Hz, 2H, 5-H), 2.76 (t, J = 7.8 Hz, 2H, 4-H). ^{13}C NMR (125 MHz: DMSO-d_6, δ): 167.28, 145.01, 134.99, 132.39, 128.37, 127.31, 126.87, 122.83, 118.25, 29.18, and 21.79.

6-Fluoro-8*H*-indeno[1,2-*d*]thiazol-2-amine (SKA-71). SKA-71 was prepared from 5-fluoro-1-indanone (1.84 g, 12.4 mmol) according to general method I. The product was isolated as lavender crystals (934 mg, 40%); m.p. = 217°C dec (CAS no. 1025800-52-5). ^{1}H NMR (500 MHz, DMSO-d_6, δ): 7.33 (doublet of triplets (dt), J = 7.9, 3.8 Hz, 2H, 4-H, and 7-H), 7.16 (s, 2H, NH_2), 7.10 (doublet of doublet of doublets (ddd), J = 10.2, 8.4, 2.5 Hz, 1H, 5-H), 3.70 (s, 2H, CH_2). ^{13}C NMR (125 MHz: DMSO-d_6, δ): 182.98, 160.95, 139.84, 128.3, 126.68, 126.53, 124.01, 114.03, 112.77, and 32.72.

5-Chloronaphtho[1,2-*d*]thiazol-2-amine (SKA-72). SKA-72 was prepared from 1-amino-4-chloronaphthalene (1.6 g, 8.8 mmol) according to general method III. The product was isolated as lavender crystals (1.27 g, 60%); m.p. = 253°C (CAS no. 1369250-74-7). ^{1}H NMR (500 MHz, DMSO-d_6, δ): 8.41 (m, 1H, 9-H), 8.14 (m, 1H, 6-H), 8.07 (s, 1H, 4-H), 7.75 (s, 2H, NH_2), 7.63 (m, 2H, 8-H, and 7-H). ^{13}C NMR (125 MHz: DMSO-d_6, δ): 168.17, 147.65, 128.19, 126.46, 126.40, 126.22, 124.82, 124.14, 123.94, 122.07, and 119.66.

4,5-Dihydroacenaphtho[5,4-*d*]thiazol-8-amine (SKA-73). SKA-73 was prepared from 1,2-dihydroacenaphthylen-5-amine (0.4 g, 2 mmol) according to general method III. The product was isolated a brown solid (400 mg, 30%); m.p. = 257°C (CAS. 108954-84-3). ^{1}H NMR (500 MHz, DMSO-d_6, δ): 7.87 (d, J = 8.2 Hz, 1H, 9-H), 7.56 (singlet (s), 1H, 4-H), 7.45 (t, J = 7.5 Hz, 1H, 8-H), 7.30 – 7.20 (m, 3H, 7-H and NH_2), 3.37 (d, J = 12.2 Hz, 4H, 4-H, and 5-H). ^{13}C NMR (125 MHz: DMSO-d_6, δ): 167.17, 146.65, 139.05, 128.19, 128.46, 124.40, 119.66, 119,24, 113.08, 31.25, and 29.92. (Note: We are following the NMR numbering designation of 2-aminobenzothiazoles, not dihydroacenaphthothiazoles.)

7,8-Dihydro-6*H*-indeno[4,5-*d*]thiazol-2-amine (SKA-81). SKA-81 was prepared from 4-aminoindan (500 mg, 3.7 mmol) according to general method III. The product was isolated as a white solid (200 mg, 30%); m.p. = 195°C. ^{1}H NMR (500 MHz, DMSO-d_6, δ): 7.38–7.37 (d, J = 7.75 Hz, 1H, 5-H), 7.25 (s, 2H, NH_2), 6.90 (d, J = 7.8 Hz, 1H, 4-H), 3.00 (t, J = 7.3, 2H, 8-H), 2.91 (t, J = 7.3 Hz, 2H, 6-H), 2.10–2.04 (q, J = 7.3 Hz, 2H, 7-H). ^{13}C NMR (125 MHz, DMSO-d_6, δ): 167.37 (2-C), 149.90 (3-C), 141.97 (4-C), 133.02 (6-C), 129.00 (8-C), 119.08 (5-C), 117.58 (4-C), 33.42 (6-C), 31.55 (8-C), 25.62 (7-C). HRMS (ESI): calculated: 191.0637; found: 191.0638.

5-Bromonaphtho[1,2-*d*]thiazol-2-amine (SKA-87). SKA-87 was prepared from 1-amino-4-bromonaphthalene (1.6 g, 8.8 mmol) according to general method III. The product was isolated as silver crystalline rods (500 mg, 45%); m.p. = 253°C (CAS. 412312-09-5). ^{1}H NMR (800 MHz, DMSO-d_6, δ): 8.40 (d, J = 8.6 Hz, 1H, 9-H), 8.24 (s, 1H, 4-H), 8.10 (d, J = 8.1 Hz, 1H, 6-H), 7.78 (s, 2H, NH_2), 7.65–7.60 (multiplet (m), 2H, 7-H, and 6-H). ^{13}C NMR (125 MHz, DMSO-d_6, δ): 168.67, 148.68, 129.71, 127.10, 127.00, 126.89, 126.88, 125.90, 124.61, 123.50, and 112.73.

Naphtho[1,2-*d*]oxazol-2-amine (SKA-102). Solid 1-amino-2-naphthol hydrochloride (0.80 g, 4 mmol) was suspended in 20 ml of dichloromethane, treated with triethylamine (0.6 ml, 20 mmol) and cyanogen bromide (3M BrCN in dichloromethane; 3 ml, 6.2 mmol), and allowed to react

overnight yielding naphtho[1,2-*d*]oxazol-2-amine HBr. To isolate the free amine, the HBr salt was suspended in ethyl acetate and free-based with ammonium hydroxide (NH_4OH). The solid residue was dissolved in a diethyl ether-ethyl acetate, treated with charcoal, and recrystallized from diethyl ether-ethyl acetate (10:1), resulting in a purple solid (100 mg, 45%); m.p. = 194°C (CAS. 858432-45-8). ^{1}H NMR (800 MHz, DMSO-d_6, δ): 8.27 (d, J = 8.3 Hz, 1H, 9-H), 7.9 (d, 1H, J = 8.16 Hz, 6-H), 7.60 (d, J = 8.88 Hz, 1H, 5-H), 7.58 (triplet (t), J = 7.92 Hz, 1H, 8-H), 7.53 (d, J = 8.72 Hz, 1H, 4-H), 7.47 (t, J = 8.01 Hz, 1H, 8-H). ^{13}C NMR (200 MHz, DMSO-d_6, δ): 163.25, 144.14, 138.53, 130.95, 128.80, 125.97, 124.72, 124.49, 121.99, 120.29, and 110.32.

5-Fluoronaphtho[1,2-*d*]thiazol-2-amine (SKA-106). SKA-106 was prepared from 4-fluoronaphthalen-1-amine (1 g, 6 mmol) according to general method III. The product was isolated as a clear oil (210 mg, 20%). ^{1}H NMR (500 MHz, acetone-d_6, δ): 8.48 (d, J = 8.1 Hz, 1H, 9-H), 8.06 (d, J = 8.2 Hz, 1H, 6-H), 7.62 (m, 3H, 8-H, 7-H, and 4-H), 6.91 (s, 2H, NH_2). ^{13}C NMR (125 MHz, acetone-d_6, δ): 167.23 (2-C), 157.95 (5-C), 145.12 (3′-C), 128.33 (6-C), 125.17 (1′-C), 126.94 (7-C), 125.80 (9-C), 125.01 (8-C) 124.29 (9′-H), 116.06 (6′-C), 103.59 (4-C). HRMS (ESI): calculated: 219.0387; found: 219.0383.

2-Aminonaphtho[1,2-*d*]thiazole-5-carbonitrile (SKA-107). SKA-107 was prepared from 4-amino-1-naphthalenecarbonitrile (1 g, 6 mmol) according to general method III. The product was isolated as a brown solid (121 mg, 45%); m.p. = 265°C. ^{1}H NMR (500 MHz, acetone-d_6, δ): 8.62 (d, J = 8.22 Hz, 1H, 9-H), 8.42 (s, 1H, 4-H), 8.20 (d, J = 8.34 Hz, 1H, 6-H), 7.78 (t, J = 7.04 Hz, 1H, 7-H), 7.73 (t, J = 7.25 Hz, 1H, 8-H), 7.48 (s, 2H, NH_2).^{13}C NMR (200 MHz, DMSO-d_6, δ): 171.82 (2-C), 153.14 (3′-C), 131.15 (6-C), 128.32 (4-C), 127.55 (9-C), 127.39 (8-C), 125.25 (7-C), 124.96 (6′-C), 124.84 (1′-C), 124.69 (9′-C), 118.94 (CN), and 99.96 (5-C). HRMS (ESI): calculated: 226.0433; found: 226.0432.

6,8-Dimethyl-4,5-dihydronaphtho[1,2-*d*]thiazol-2-amine (SKA-108). SKA-108 was prepared from 5,7-dimethyl-1-tetralone (2 g, 11 mmol) according to general method I. The product was isolated as pink crystals (300 mg, 16%); m.p. = 159°C. ^{1}H NMR (500 MHz, acetone-d_6, δ): 7.40 (s, 1H, 9-H), 6.83 (s, 1H, 7-H), 6.17 (s, 2H, NH_2), 2.91 (t, J = 7.87 Hz, 2H, 4-H), 2.81 (t, J = 7.56 Hz, 2H, 5-H), 2.27 (s, 3H, 8-CH_3), 2.25 (s, 3H, 6-CH_3). ^{13}C NMR (200 MHz, DMSO-d_6, δ): 166.86 (2-C), 145.13 (3′-C), 135.11 (8-C), 135.09 (6-C), 131.86 (6′-H), 129.81 (7-H), 129.41 (9′-C), 121.69 (9-C), 117.36 (1′-C), 28.8 (4-CH_2), 24.57 (5-CH_2), 21.37 (8-CH_3), and 19.88 (6-CH_3). HRMS (ESI): calculated: 231.0950; found: 231.0949.

6,8-Dimethylnaphtho[1,2-*d*]thiazol-2-amine (SKA-109). SKA-109 was prepared from 5,7-dimethyl-1-tetralone (2 g, 11 mmol) according to general method II. The product was isolated as pink crystals (15 mg, 0.6%); m.p. = 157°C. ^{1}H NMR (500 MHz, DMSO-d_6, δ): 8.02 (s, 1H, 9-H), 7.73 (d, J = 8.81 Hz, 1H, 4-H), 7.59 (d, J = 8.84 Hz, 1H, 5-H), 7.53 (s, 2H, NH_2), 7.17 (s, 1H, 7-H), 2.61 (s, 3H, 8-CH_3), 2.45 (s, 3H, 6-CH_3). ^{13}C NMR (125 MHz, DMSO-d_6, δ): 167.84 (2-C), 148.80 (3′-C), 135.61 (8-C), 134.92 (6-C), 128.70 (7-C), 126.90 (9-C), 121.68 (6′-C), 118.78 (1′-C), 117.57 (4-C), 100.61 (9′-C), 99.85 (5-C), 22.21 (8-CH_3), and 20.14 (6-CH_3). HRMS (ESI): calculated: 222.0794; found: 222.0794.

Thieno[2′,3′:5,6]benzo[1,2-*d*]thiazol-2-amine (SKA-110). SKA-110 was prepared from 6,7-dihydro-4-benzo[*b*]thiophenone (0.5 g, 3 mmol) according to general procedure II. The product was isolated as a white solid (26 mg, 3.8%), m.p. = 161°C (CAS. 35711-03-6). ^{1}H NMR (800 MHz, DMSO-d_6, δ): 7.71 (d, J = 5.36 Hz, 1H, 7-H), 7.68 – 7.62 (m, 4H, 4-H, 5-H, and NH_2), 7.58 (d, J = 5.41 Hz, 1H, 6-H). ^{13}C NMR (125 MHz, DMSO-d_6, δ): 168.26, 147.81, 137.83, 131.22, 126.97, 125.72, 121.95, 117.97, and 115.51.

5-Methylnaphtho[1,2-*d*]thiazol-2-amine (SKA-111). SKA-111 was prepared from 4-methyl-1-tetralone (1 g, 11 mmol) according to general procedure II. The product was isolated as yellow crystals (100 mg, 16%); m.p. = 209°C (CAS. 1369170-24-0). ^{1}H NMR (800 MHz, DMSO-d_6, δ): 8.96 (d, J = 7.86 Hz, 1H, 9-H), 8.46 (d, J = 7.99 Hz, 1H, 6-H), 8.06 (s, 1H, 4-H), 7.98 (dt, J = 6.83, 13.83 Hz, 2H, 7-H and 8-H), 7.16 (s, 2H, NH_2), 3.14 (s, 3H, CH_3).^{13}C NMR (125 MHz, DMSO-d_6, δ): 166.73, 147.60, 131.54, 127.88, 127.33, 126.02, 125.58, 125.27, 124.75, 124.70, 119.39, and 19.01.

8-Fluoronaphtho[1,2-*d*]thiazol-2-amine (SKA-112). SKA-112 was prepared from 7-fluoro-1-tetralone (0.5 g, 3 mmol) according to general procedure II. The product was isolated a clear oil (10 mg, 3%). ^{1}H NMR (500 MHz, DMSO-d_6, δ): 8.00 (dd, J = 5.74, 9.02 Hz, 1H, 7-H), 7.90 (dd, J = 2.67, 10.46 Hz, 1H, 9-H), 7.79 (d, J = 8.61 Hz, 1H, 5-H), 7.67 (s, 2H, NH_2), 7.60 (d, J = 8.64 Hz, 1H, 4-H), 7.37 (triplet of doublets (td), J = 2.73, 8.83 Hz, 1H, 6-H). ^{13}C NMR (125 MHz, DMSO, δ): 168.40 (2-C), 161.60 (8-CF), 159.67 (3′-C), 148.183 (6-C), 131.73 (6′-C), 129.52 (1′-C), 126.84 (9′-C), 121.27 (7-C), 119.43 (4-C), 115.54 (5-C), and 107.29 (9-C). HRMS (ESI): calculated: 219.0387; found: 219.0383.

5-Methyl-4,5-dihydronaphtho[1,2-*d*]thiazol-2-amine (SKA-113). SKA-113 was prepared from 4-methyl-1-tetralone (2 g, 11 mmol) according to general procedure I. The product was isolated as white crystals (250 mg, 20%); m.p. = 109°C dec (CAS no. 896156-31-3). ^{1}H NMR (500 MHz, DMSO-d_6, δ): 7.56 (d, J = 6.4 Hz, 1H, 9-H), 7.40 (s, 2H, NH_2), 7.21 (m, 3H, 6-H, 7-H, and 8-H), 3.12 (h, J = 6.8 Hz, 1H, 5-H), 2.76 (ddd, J = 175.4, 16.2, 6.6 Hz, 2H, 4-CH_2), 1.23 (d, J = 6.9 Hz, 3H, 5-CH_3). ^{13}C NMR (125 MHz, DMSO-d_6, δ): 167.85, 152.42, 140.02, 127.69, 127.37, 127.29, 122.97, 116.67, 99.85, 33.48, 29.20, and 21.45.

6-Methoxy-4,5-dihydronaphtho[1,2-*d*]thiazol-2-amine (SKA-114). SKA-114 was prepared from 5-methoxy-1-tetralone (2 g, 11 mmol) according to general procedure I. The product was isolated as brown crystals (1.5 g 57%); m.p. = 200°C (CAS no. 489430-53-7). ^{1}H NMR (500 MHz, DMSO-d_6, δ): 7.23–7.13 (m, 2H, 9-H, and 8-H), 6.91 (s, 2H, NH_2), 6.84 (d, J = 7.59 Hz, 1H, 7-H), 3.79 (s, 3H, OCH_3), 2.89 (t, J = 8.09 Hz, 2H, 4-CH_2), 2.73 (t, J = 8.07 Hz, 2H, 5-CH_2). ^{13}C NMR (125 MHz, DMSO-d_6, δ): 167.04, 156.69, 144.90, 133.25, 127.75, 122.02, 118.20, 115.94, 110.01, 56.10, 21.50, and 21.18.

5-Methoxynaphtho[1,2-*d*]thiazol-2-amine (SKA-117). SKA-117 was prepared from 1-amino-4-methoxynaphthalene (0.1 g, 0.51 mmol) according to general method III. The product was isolated as lavender crystals (16 mg, 14%); m.p. = 213°C (CAS. 1368289-59-1). ^{1}H NMR (500 MHz, DMSO-d_6, δ): 8.87 (d, J = 8.25 Hz, 1H, 9-H), 8.68 (d, J = 8.3 Hz, 1H, 6-H), 8.02 (t, J = 7.4 Hz, 1H, 7-H), 7.95 (t, J = 7.4 Hz, 1H, 8-H), 7.56 (s, 1H, 4-H), 7.11 (s, 2H, NH_2), 4.49 (s, 3H, OCH_3). ^{13}C NMR (125 MHz, DMSO-d_6, δ): 168.11, 155.81, 148.63, 127.48, 126.6, 126.56, 123.94, 119.16, 116.51, 114.98, 104.55, and 56.26.

5-Methylnaphtho[1,2-*d*]oxazol-2-amine (SKA-120). SKA-120 was prepared from 4-methyl-1-tetralone according to general procedure IV. The product was isolated as light brown crystals (50 mg, 4%); m.p. = 209°C; R_f = 0.38 (cyclohexane-EtOAc, 1:1). ^{1}H NMR (800 MHz, $CDCl_3$, δ): 8.28 (d, J = 8.3 Hz, 1H, 9-H), 8.03 (d, J = 8.4 Hz, 1H, 6-H), 7.58 (t, J = 7.4 Hz, 1H, 8-H), 7.52 (t, J = 7.5 Hz, 1H, 7-H), 7.38 (s, 1H, 4-H), 5.39 (bs, 2H, NH_2), and 2.74 (s, 3H, CH_3). ^{13}C NMR (200 MHz, $CDCl_3$, δ): 160.37 (2-C), 152.05 (1′-C), 135.20 (3′-C), 130.07 (9′-C), 129.14 (6′-C), 126.12 (8-C), 125.33 (5-C), 124.91 (6-C), 124.77 (7′-C), 122.38 (9-C), 110.56 (4-C), 19.93 (5-CH_3). ^{1}H,^{13}C-HSQC (800 MHz, $CDCl_3$, cross-peaks δ): 8.28/122.38, 8.03/124.91, 7.58/126.12, 7.51/124.77, 7.38/110.57, and 2.80/19.93. HRMS (ESI): calculated: 199.0866; found: 199.0864.

5-Methylnaphtho[2,1-*d*]oxazol-2-amine (SKA-121). SKA-121 was prepared from 4-methyl-1-tetralone according to general procedure IV. The product was isolated as brown crystals (50 mg, 4%); m.p. = 186°C dec; R_f = 0.28 (cyclohexane-EtOAc, 1:1). ^{1}H NMR (800 MHz, $CDCl_3$, δ): 8.03 (d, J = 8.5 Hz, 1H, 9-H), 8.01 (d, J = 8.3 Hz, 1H, 6-H), 7.56 (t, J = 7.5 Hz, 1H, 7-H), 7.45 (t, J = 6.0 Hz, 1H, 8-H), 7.43 (s, 1H, 4-H), 5.33 (bs, 2H, NH_2), 2.73 (s, 3H, CH_3). ^{13}C NMR (200 MHz, $CDCl_3$, δ): 160.80 (2-C), 141.72 (1'-C), 137.24 (3′-C), 128.85 (5-C), 119.28 (6-C), 125.21 (9-C), 126.39 (7-C), 123.92 (8-C), 131.34 (6′-C), 119.77 (9′-C), 117.17 (4-C), 19.58 (5-CH_3). ^{1}H,^{13}C-HSQC (800 MHz, $CDCl_3$, cross-peaks δ): 8.03/125.21, 8.01/119.28, 7.56/126.39, 7.45/123.92, 7.43/117.17, and 2.73/19.58. HRMS (ESI): calculated: 199.0866; found: 199.0864.

Crystal Structure Determinations

The SKA-120 and SKA-121 crystals selected for data collection were mounted in the 90-K nitrogen cold stream provided by a CRYO Industries of America (Manchester, NH) low-temperature apparatus

on the goniometer head of a Bruker D8 diffractometer equipped with an ApexII CCD detector (Bruker, Fremont, CA). Data were collected with the use of Mo Kα radiation (λ = 0.71073 Å). The structures were solved by direct methods (SHELXS-97) and refined by full-matrix least-squares on F^2 (SHELXL-2013). All nonhydrogen atoms were refined with anisotropic displacement parameters. For a description of the method, see Sheldrick (2008).

Crystal Data SKA-120. $C_{12}H_{10}N_2O$, F.w. = 198.22, brown plate, dimensions 0.18 × 0.34 × 0.60 mm, monoclinic, $P2_1/n$, a = 14.2110(9) Å, b = 3.8854(3) Å, c = 17.5101(11) Å, β = 107.537(2)°, V = 921.89(11) Å^3, Z = 4, $R1$ [1518 reflections with $I > 2\sigma(I)$] = 0.0307, $wR2$ (all 1671 data) = 0.0900, 176 parameters, 0 restraints.

Crystal Data SKA-121. $C_{12}H_{10}N_2O$, F.w. = 198.22, brown plate, monoclinic, $P2_1/n$, a = 8.0532(12) Å, b = 21.377(3) Å, c = 11.5094(17) Å, β = 107.823(2)°, V = 1886.3(5) Å^3, Z = 8, $R1$ [2571 reflections with $I > 2\sigma(I)$] = 0.0376, $wR2$ (all 3413 data) = 0.0949, 335 parameters, 0 restraints.

CCDC 9966657 and 996658 contains the supplemental crystallographic data for this article. These data can be obtained free of charge from The Cambridge Crystallographic Data Centre via www.ccdc.cam.ac.uk/data_request/cif.

Cells, Cell Lines, and Clones

Human embryonic kidney cells (HEK-293) stably expressing hK_{Ca}2.1, rK_{Ca}2.2, and hK_{Ca}3.1 were obtained from Khaled Houamed (University of Chicago, IL) in 2002 and have been maintained in the Wulff Laboratory at the University of California since then. The cloning of hK_{Ca}2.3 (19 CAG repeats) and hK_{Ca}3.1 was previously described (Wulff et al., 2000). The hKCa2.3 clone was later stably expressed in COS-7 cells at Aurora Biosciences Corp. (San Diego, CA). Cell lines stably expressing other mammalian ion channels were gifts from several sources: hK_{Ca}1.1 in HEK-293 cells (Andrew Tinker, University College London); hK_V2.1 in HEK293 cells (James Trimmer, University of California Davis, Davis, CA); K_V11.1 (HERG) in HEK-293 cells (Craig January, University of Wisconsin, Madison); hNa_V1.4 in HEK-293 cells (Frank Lehmann-Horn, University of Ulm, Germany); hNa_V1.5 in HEK-293 cells (Christopher Lossin, University of California Davis); and hCa_V1.2 in HEK-293 cells (Franz Hofmann, Munich, Germany). L929 cells stably expressing mK_V1.3 and mK_V3.1 have been previously described (Grissmer et al., 1994); N1E-115 neuroblastoma cells (expressing mNa_V1.2) were obtained from ATCC; division arrested CHO cells expressing hNa_V1.7 were purchased from ChanTest (Cleveland, OH).

Electrophysiology

Experiments were conducted either manually with an EPC-10 amplifier (HEKA, Lambrecht/Pfalz, Germany) or on a QPatch-16 automated electrophysiology platform (Sophion Biosciences, Ballerup, Denmark). For manual experiments, COS-7, HEK-293, or L929 cells were trypsinized, plated onto poly-L-lysine–coated coverslips, and typically recorded from between 20 minutes and 4 hours after plating. Patch pipettes were pulled from soda lime glass (micro-hematocrit tubes, Kimble Chase, Rochester, NY) and had resistances of 2-3 MΩ. For measurements of K_{Ca} channels expressed in HEK-293 cells (K_{Ca}2.1, K_{Ca}2.2, and K_{Ca}3.1), we used normal Ringer solution as external with an internal pipette solution containing (in mM): 140 KCl, 1.75 $MgCl_2$, 10 HEPES, 10 EGTA, and 7.4 $CaCl_2$ (500 nM free Ca^{2+}) or 6 $CaCl_2$ (250 nM free Ca^{2+}), pH 7.2, 290–310 mOsm. Free Ca^{2+} concentrations were calculated with MaxChelator assuming a temperature of 25°C, a pH of 7.2, and an ionic strength of 160 mM. To reduce contaminating currents from native chloride channels in COS-7 cells, K_{Ca}2.3 currents were recorded with an internal pipette solution containing (in mM) the following: 145 K^+ aspartate, 2 $MgCl_2$, 10 HEPES, 10 EGTA, and 7.4 $CaCl_2$ (500 nM free Ca^{2+}), pH 7.2, 290–310 mOsm. Na^+ aspartate Ringer was used as an external solution (in mM): 160 Na^+ aspartate, 4.5 KCl, 2 $CaCl_2$, 1 $MgCl_2$, 5 HEPES, pH 7.4, 290–310 mOsm. Both K_{Ca}2 and K_{Ca}3.1 currents were elicited by 200-ms voltage ramps from −120 mV to 40 mV applied every 10 seconds, and the -fold increase of slope conductance at −80 mV by drug taken as a measure of channel activation. K_V2.1, K_V1.3, and K_V3.1 currents were recorded in normal Ringer solution with a Ca^{2+}-free KF-based pipette solution as previously described (Schmitz et al., 2005). HERG (K_V11.1) currents were recorded with a two-step pulse from −80 mV first, to 20 mV for 1 second, and then to −50 mV for a 1-second reduction of both peak and tail current by the drug. Na_V1.7 currents were recorded with 30-millisecond pulses from −90 mV to 10 mV every 10 seconds with a CsF-based pipette solution and normal Ringer as an external solution. Ca_V1.2 currents were elicited by 100-millisecond depolarizing pulses from −80 to 20 mV every 10 seconds with a CsCl-based pipette solution and an external solution containing 30 mM $BaCl_2$. Blockade of both Na^+ and Ca^{2+} currents was determined as reduction of the current minimum.

For automated electrophysiology experiments, cells were grown to ~70% confluency, rinsed in sterile phosphate-buffered saline containing 0.02% EDTA, and lifted with 2 ml of TrypLE Express (Gibco, Grand Island, NY) for ~2 minutes. When cells were rounded but not detached, they were dislodged by gentle tapping, suspended in Dulbecco's modified Eagle's medium, centrifuged, and resuspended in 1 ml of external solution; placed into the Qfuge tube; and resuspended in 150–200 μl of extracellular solution after one additional spin on the QPatch. Whole-cell patch-clamp experiments were then carried out using disposable 16-channel planar patch chip plates (QPlates; patch-hole diameter approximately 1 μm, resistance 2.00 ± 0.02 MΩ). Cell positioning and sealing parameters were set as follows: positioning pressure −70 mbar, resistance increase for success 750%, minimum-seal resistance 0.1 GΩ, holding potential −80 mV, and holding pressure −20 mbar. To avoid the rejection of cells with large K_{Ca}3.1 currents, the minimum seal resistance for whole-cell requirement was lowered to 0.001 GΩ. Access was obtained with the following sequence: 1) suction pulses in 29-mbar increments from −250 mbar to −453 mbar; 2) a suction ramp of an amplitude of −450 mbar; 3) 400-mV voltage zaps of 1-milliseconds' duration (10×). After establishment of the whole-cell configuration, cells were held at −80 mV and K_{Ca}3.1, K_{Ca}2.1, or K_{Ca}2.2 currents elicited by a voltage protocol that held at −80 mV for 20 ms, stepped to −120 mV for 20 milliseconds, ramped from −120 to 40 mV in 200 milliseconds, and then stepped back to −120 mV for 20 milliseconds. This pulse protocol was applied every 10 seconds. K_{Ca}1.1 currents were elicited by 160-ms voltage ramps from −80 to 80 mV applied every 10 seconds (500 nM free Ca^{2+}), and channel modulation was measured as a change in mean current amplitude. Na_V1.2 currents from N1E-115 cells, Na_V1.4, and Na_V1.5 currents from stably transfected HEK cells were recorded with 20-millisecond pulses from −90 mV to 0 mV every 10 seconds with a KF-based internal solution and normal Ringer as an external solution. Current slopes (in ampere per sec) were measured using the Sophion QPatch software and exported to Microsoft Excel and Origin 7.0 (OriginLab Corp., Northampton, MA) for analysis. Increases or decreases of slopes between −85 and −65 mV were used to calculate K_{Ca}2/3 activation. Data fitting to the Hill equation to obtain EC_{50} and IC_{50} values were performed with Origin 7.0. Data are expressed as mean ± S.D.

The inside-out experiments shown in Fig. 4 were performed on the K_{Ca}3.1-stable HEK 293 cell line. Symmetrical K^+ was used to obtain larger currents. The extracellular solutions contained (in mM) the following: 154 KCl, 10 HEPES (pH = 7.4), 2 $CaCl_2$, and 1 $MgCl_2$. Solutions on the intracellular side contained (in mM) the following: 154 KCl, 10 HEPES (pH = 7.2), 10 EGTA, 1.75 $MgCl_2$, and $CaCl_2$ to yield calculated free Ca^{2+}-concentrations of 0.05, 0.1, 0.25, 0.3, 0.5, 1.0, and 10.0 μM. Cells were clamped to a holding potential of at 0 mV, and K_{Ca} currents were elicited by 200-millisecond voltage ramps from −80 to 80 mV applied every 10 seconds.

For all electrophysiology experiments, solutions of benzothiazoles and benzooxazoles were always freshly prepared from 1 mM or 10 mM stock solutions in DMSO during the experiment. The final DMSO concentration never exceeded 1%. For automated assays, glass vial inserts (Sophion Biosciences) were filled with 350–400 μl of compound

solution and placed into the glass insert base plate for use in the QPatch assay right before starting the QPatch.

Isometric Myography on Porcine Coronary Arteries

Porcine coronary arteries (PCAs) were carefully dissected from hearts kindly provided by the local abattoir (Mercazaragoza, Zaragoza, Spain), cleaned of fat and connective tissue, and cut into 3- to 4-mm rings. Rings were mounted on hooks connected to an isometric force transducer (Pioden UF1, Graham Bell House, Canterbury, UK) and prestretched to an initial tension of 1 g. Composition Krebs' buffer (in mM) was as follows: NaCl 120, $NaHCO_3$ 24.5, $CaCl_2$ 2.4, KCl 4.7, $MgSO_4$ 1.2, KH_2PO_4 1, and glucose 5.6, pH 7.4, at 37°C and equilibrated with 95% O_2/5% CO_2. Changes in tension were registered using a Mac Laboratory System/8e program (AD Instruments Inc., Milford, MA). The buffer contained the NO-synthase blocker, Nω-nitro-L-arginine (L-NNA, 300 μM), and the cyclooxygenase blocker indomethacin (10 μM) to measure EDH-type relaxation. After three washes, rings were precontracted with the thromboxane analog U46619 (0.2 μM). Thereafter rings were exposed to bradykinin (BK, 1 μM) in combination with vehicle DMSO, SKA-111 (1 μM), SKA-111 plus TRAM-34 (1 μM), SKA-111 plus TRAM-34 plus UCL-1684 (1 μM), SKA-121 (1 μM), SKA-121 plus TRAM-34, or SKA-121 plus TRAM-34 plus UCL-1684. After washout, rings were contracted with a high KCl buffer (60 mM) to determine maximal contraction. TRAM-34 was synthesized as previously described (Wulff et al., 2000). UCL1684 and U46619 were purchased from Tocris (Wiesbaden-Nordenstadt, Germany). Data analysis was as follows: EDH-type relaxations were determined as percentage of change of U46619 contraction and are shown relative to the totally relaxed state (without U46619).

Telemetry

The experiments were in accordance with the Animal Research Reporting In Vivo Experiments guidelines and approved by the Institutional Animal Care and Use Committee of the IACS. Surgical implantation of TA11PA-C10 pressure transducers (Data Sciences International, St. Paul, MN) into the left carotid artery and telemetry were performed as described previously (Brahler et al., 2009). Four female wild-type (22 ± 1 g) and four female $KCa3.1^{-/-}$ (27 ± 2 g) mice were used in the present study. After surgery, mice were allowed to recover for 10 days before compounds or vehicle were injected and telemetry data were collected. After a washout phase of at least 48 hours after a first injection, animals were reused for injections of a higher dose of the SKA-111, SKA-121, or vehicle. Thereafter, mice were treated with 50 μg/ml Nω-nitro-L-arginine methyl ester (L-NAME, Sigma-Aldrich DK) in the drinking water. This L-NAME treatment over 2 days increased MAP by 10 ± 2 mm Hg in wild-type mice. Injection of compounds started on day 3 of L-NAME treatment. Preparation and injection of SKA-111 and SKA-121 were as follows: Appropriate amounts of SKA-111 and SKA-121 were dissolved in warmed peanut oil (SKA-111) or in a mixture of peanut oil/DMSO (9:1 v/v, both from Sigma-Aldrich DK) to give a dose of 30 or 100 mg/kg. Maximal injection volume was ±600 μl. SKA-111 solution, well-stirred suspension (SKA-121), or vehicle was injected i.p. during hour 3 of the dark phase. Mice were subjected to isoflurane anesthesia to minimize stress and pain during compound application. Telemetry data were collected and analyzed after the mice fully recovered from anesthesia (20 minutes after injection). Telemetry data were recorded over 1 minute every 10 minutes over 24 hours and averaged. Data were analyzed using Data Sciences International software.

Pharmacokinetics

Twelve-week-old male C57Bl/6J mice were purchased from Charles River Laboratories (Wilmington, MA) and housed in microisolator cages with rodent chow and autoclaved water ad libitum. All experiments were in accordance with National Institutes of Health guidelines and approved by the University of California, Davis Institutional Animal Care and Use Committee. For i.v. application, SKA-111 and SKA-121 were dissolved at 5 mg/ml in a mixture of 10% CremophorEL (Sigma-Aldrich, St. Louis, MO) and 90% phosphate-buffered saline and then injected at 10 mg/kg into the tail vein (n = 8 mice per compound). Another group of mice (n = 8) received SKA-121 orally. At various time points after the injection, blood was collected into EDTA blood sample collection tubes either from the saphenous vein or by cardiac puncture under deep isoflurane anesthesia. After the cardiac puncture, mice were sacrificed by cutting the heart, and then the brain was removed. Individual mice were typically used for three times points (two blood collections from the saphenous vein plus the terminal blood collection). Plasma was separated by centrifugation, and plasma and brain samples were stored at −80°C pending analysis. Brain samples were homogenized in 1 ml of H_2O with a Brinkman Kinematica PT 1600E homogenizer, and the protein was precipitated with 1 ml of acetonitrile. The samples were then centrifuged at 3000 rpm, and supernatants concentrated to 1 ml. Plasma and homogenized brain samples were purified using C18 solid-phase extraction cartridges (ThermoFisher Scientific, Waltham, MA) preconditioned with acetonitrile, followed by 1 ml of water. The loaded column was washed with 2 ml of water. SKA-121 was eluted with 3 ml of acetonitrile. SKA-111 was eluted with 3 ml of methanol containing 1% NH_4OH. Eluted fractions were dried under nitrogen and reconstituted in acetonitrile. LC/MS analysis was performed with a Waters Acquity UPLC (Waters, New York, NY) equipped with a Acquity UPLC BEH 1.7 μm RP-18 column (Waters, New York, NY) interfaced to a TSQ Quantum Access Max mass spectrometer (MS) (ThermoFisher Scientific, Waltham, MA). The isocratic mobile phase consisted of 80% acetonitrile and 20% water, both containing 0.1% formic acid with a flow rate of 0.25 ml per minute. Under these conditions SKA-111 had a retention time of 0.83 minute and SKA-121 a retention time of 0.96 minute. Using electrospray ionization, MS and selective reaction monitoring (capillary temperature 300°C, capillary voltage 4000 V, collision energy -34 eV, positive ion mode), SKA-121 was quantified by its base peak of 128.14 m/z and its concentration was calculated with a 5-point calibration curve from 100 nM to 10 μM. SKA-111 (capillary temperature 325°C, capillary voltage 4000 V, collision energy −28eV, positive ion mode) was quantified by its base peak of 200.045 m/z and its concentration was calculated with a six-point calibration curve from 100 nM to 20 μM.

The percentage of plasma protein binding for SKA-111 and SKA-121 was determined by ultrafiltration. Rat plasma (500 μl) was spiked with 10 μM of compound in 1% DMSO, and the sample was loaded onto a Microcon YM-30 Centrifugal Filter (Millipore Corp., Bedford, MA) and centrifuged at 13,500g for 30 minutes at RT. The retentate was collected by inverting the filter into an Eppendorf tube and spinning at 13,500g for 15 minutes. The retentate then underwent sample preparation as per the previously described procedure for SKA-111 or SKA-121. Plasma protein binding was found to be to be 59 ± 2% (n = 3) for SKA-111 and 81 ± 4% (n = 2) for SKA-121.

Results

SAR Study Aiming to Obtain Selectivity for $K_{Ca}3.1$ with SKA-31 as a Template. As described in the *Introduction*, the limited ability of existing benzimidazole/benzothiazole-type $K_{Ca}2/3$ activators such as SKA-31 to differentiate between $K_{Ca}2$ and $K_{Ca}3.1$ channels made it desirable to determine whether additional structural modification would increase selectivity for $K_{Ca}3.1$. Toward this goal, we synthesized a small focused library of 2-aminothiazoles, 2-aminobenzothiazoles or 2-aminonapthooxazoles (Fig. 1). Substituted 2-aminothiazoles were prepared by a one-step Hantzsch thiazole synthesis (Goblyos et al., 2005) from the appropriate substituted 1-tetralone, thiourea, and iodine (Method I in Fig. 1). This method allowed us to obtain both "open" 2-aminothiazoles as well as to

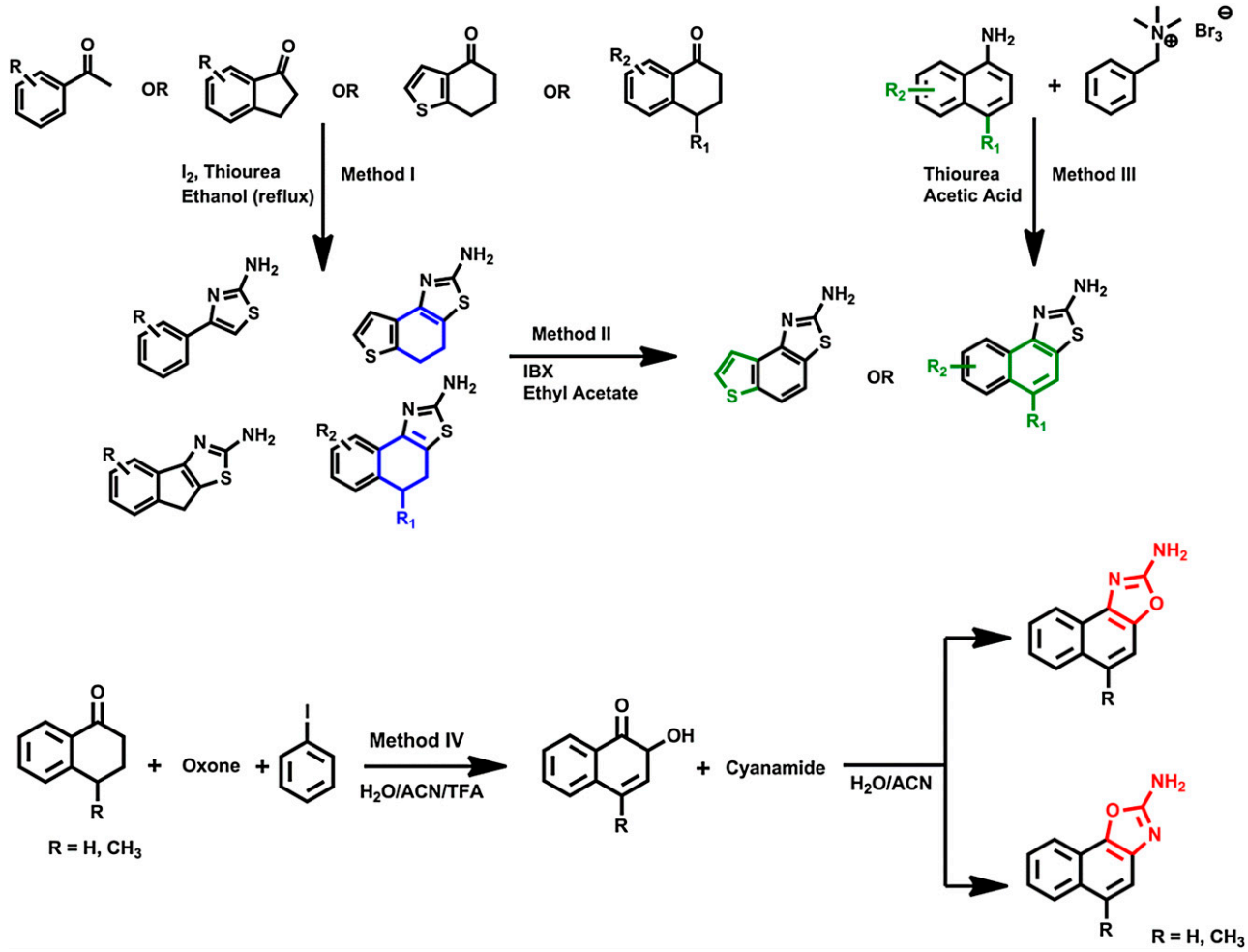

Fig. 1. General scheme for the synthesis of thiazoles, 2-aminonaphtho[1,2-*d*]thiazoles, and 2-aminonaphtho[1,2-*d*]oxazoles.

replace the central aromatic ring of SKA-31 with aliphatic rings. Fully aromatic 2-aminobenzothiazoles could then be produced by aromatizing with 2-iodoxybenzoic acid (Method II in Fig. 1). An alternative route to 5-position substituted 2-aminobenzothiazole was the classic Hugerschoff benzothiazole synthesis (Jordan et al., 2003), in which appropriately substituted amines were transformed into the corresponding thioureas and then subsequently reacted with benzyltrimethyl ammonium tribromide to deliver bromine in stoichiometric amounts as an alternative to liquid bromine (Method III in Fig. 1). Lastly, naphthooxazoles were prepared by first oxidizing 4-methyl-1-tetralone with in situ formed bis(trifluoroacetoxy)iodo] benzene and then adding cyanamide (Schuart and Müller, 1973) to the intermediately produced 4-methylnaphthalene-1,2-dione (Method IV in Fig. 1).

The compounds synthesized by these methods as well as five commercially available compounds were tested for their $K_{Ca}2.3$- and $K_{Ca}3.1$-activating activity using either manual or automated whole-cell patch-clamp. Our group previously described the establishment of a QPatch assay for $K_{Ca}3.1$ modulators. In this study, we benchmarked data obtained on the QPatch against manual patch-clamp electrophysiology by determining the potency of several commonly used $K_{Ca}3.1$ inhibitors (TRAM-34, NS6180, charybdotoxin) and activators (EBIO, riluzole, SKA-31) and found that the QPatch results were virtually identical to the IC_{50} and EC_{50} values obtained by manual patch clamp in our hands (Jenkins et al., 2013). We here made use of this assay and determined EC_{50} values for $K_{Ca}3.1$ activation using HEK-293 cells stably expressing human $K_{Ca}3.1$. Activities on human $K_{Ca}2.3$ were determined by manual electrophysiology since we currently only have $K_{Ca}2.3$ available in COS-7 cells, which are difficult to handle on the QPatch. For both channels we used 250 nM of free $[Ca^{2+}]_i$ since positive gating-modulators like SKA-31 typically increase K_{Ca} currents at this Ca^{2+} concentration roughly 30-fold, creating a large assay window (Sankaranarayanan et al., 2009; Jenkins et al., 2013).

Removal of the continuous conjugation by opening of the napthothiazole system (SKA-75 and SKA-76) of SKA-31 or replacement of the internal aromatic ring with either a cyclohexyl (SKA-70, SKA-108, SKA-113, SKA-114) or a cyclopentyl ring (SKA-69, SKA-71) in general reduced both potency and selectivity irrespective of whether the compounds bore any substituents or not (Fig. 2, blue compounds). Since these results demonstrated that aromaticity of the internal ring was required for both $K_{Ca}2.3$ and $K_{Ca}3.1$ activation, we went back to benzothiazoles (Fig. 2 green compounds) and next explored substitutions on the napthothiazole system of SKA-31. Introduction

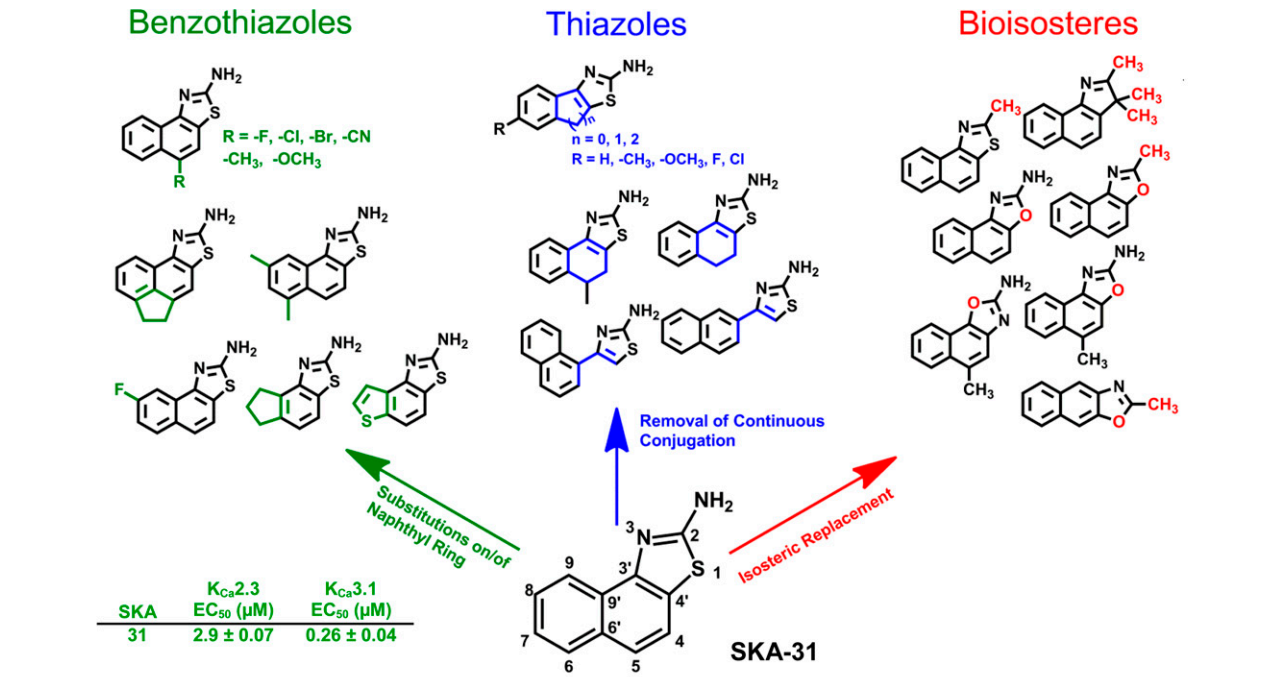

SKA	$K_{Ca}2.3$ EC_{50} (μM)	$K_{Ca}3.1$ EC_{50} (μM)
31	2.9 ± 0.07	0.26 ± 0.04

SKA	$K_{Ca}2.3$ EC_{50} (μM)	$K_{Ca}3.1$ EC_{50} (μM)
72 Cl	0.335 ±0.25	0.110 ± 0.10
106 F	29 ± 6.6	2 ± 0.39
87 Br	Insoluble	Insoluble
111 CH_3	13.7 ± 6.9	0.111 ± 0.027
117	N.D.	0.9 ± 0.4
107	2.1 ± 0.3	1.2 ± 0.3
109	>50 μM	2.4 ± 0.3
73	1.5 ± 0.9	1.1 ± 0.1
112	7.2 ± 3.0	4.6 ± 2.7
110	35 ± 11	1.2 ± 0.3
81	5.0 ± 1.7	0.711 ± 0.67

SKA	$K_{Ca}2.3$ EC_{50} (μM)	$K_{Ca}3.1$ EC_{50} (μM)
75	17 ± 8.6	21 ± 5.9
76	24 ± 8.2	>50 μM
70	> 50 μM	2.1 ± 0.5
108	24 ± 5.9	2.0 ± 0.5
113	7.2 ± 0.86	1.0 ± 0.1
114	24 ± 5.9	3.8 ± 0.34
69	27 ± 1.5	20 ± 2.3
71	> 50 μM	15 ± 0.2

SKA	$K_{Ca}2.3$ EC_{50} (μM)	$K_{Ca}3.1$ EC_{50} (μM)
74	>50 μM	7.8 ± 1.8
103	>50 μM	>50 μM
104	N.D.	>50 μM
92	>50 μM	>50 μM
102	24 ± 5.2	2.7 ± 0.15
120	9.2 ± 0.3	0.179 ± 0.03
121	4.4 ± 0.2.3	0.109 ± 0.014

N.D. not determined

Fig. 2. Chemical structures and EC_{50} values for $K_{Ca}2.3$ and $K_{Ca}3.1$ activation. All compounds were tested at least three times at concentrations of 4 to 5, and EC_{50} values were determined by fitting the Hill equation to the increase in slope conductance between −80 and −65 mV.

of substituents in the 5-position had varying effects: chloride (SKA-72), which is both electron withdrawing and lipophilic, increased potency on both $K_{Ca}2.3$ (EC_{50} 335 nM) and $K_{Ca}3.1$ (EC_{50} 110 nM) but basically abolished any selectivity between the two channels. Fluoride in the 5-position (SKA-106) reduced potency roughly 10-fold compared with SKA-31 but preserved selectivity, whereas introduction of bromide (SKA-87) resulted in a compound that was too insoluble to be tested. Introduction of a methyl group in the 5-position, which is less lipophilic than chloride but has a positive inductive effect on the ring system, slightly increased potency for $K_{Ca}3.1$ (EC_{50} 111 nM) in comparison with SKA-31 and dramatically increased selectivity for $K_{Ca}3.1$ over $K_{Ca}2.3$ to ~100-fold (SKA-111). However, replacement of the CH_3 group with other, larger

carbon containing electron-donating groups such as $-OCH_3$ (SKA-117) or electron withdrawing groups such as –CN (SKA-107) again reduced potency and selectivity. Attaching two of the obviously favorable CH_3 groups in positions 6 and 8 of the ring system (SKA-109) instead of the 5-position preserved selectivity over $K_{Ca}2.3$ but reduced potency on $K_{Ca}3.1$ by 10-fold. Installation of an ethylene bridge connecting the 5- and 6- position reduced both potency and selectivity and resulted in a compound (SKA-73) that activated both $K_{Ca}2.3$ and $K_{Ca}3.1$ equipotently with an EC_{50} of 1 μM. We further tried replacing the terminal ring of SKA-31 with a thiophene (SKA-110) or an aliphatic cyclopentyl (SKA-81) but again only saw a reduction in potency.

To better understand the full extent of the pharmacophore and potentially obtain patentable compounds, we explored alternative scaffolds (Fig. 2, red compounds). Moving away from the 2-aminothiazole system by replacing the 2-position NH_2 group with a CH_3 group (SKA-74), as well as isosterically replacing the S atom with an O (SKA-103 and SKA-104) or geminal CH_3 groups (SKA-92), completely abolished activity. However, if the 2-position NH_2 group was retained and only the S isosterically replaced with an O as in the SKA-102, which basically constitutes an oxazole analogous SKA-31, activity was regained, and the resulting compound activated $K_{Ca}3.1$ with an EC_{50} of 2.7 μM. Introduction of a CH_3 group in 5-position, which previously was found to increase selectivity of the napthothiazole SKA-111 for $K_{Ca}3.1$ to 100-fold, had a similar effect on the 2-aminonaphthooxazole system. The two regioisomers, SKA-120 and SKA-121, which resulted from the synthesis and had to be separated by flash chromatography, exhibited EC_{50} values of 180 and 109 nM for $K_{Ca}3.1$ and EC_{50} values of 9.2 and 4.4 μM for $K_{Ca}2.3$, corresponding to a ~50- or 40-fold selectivity. The correct structural assignment of the two regioisomers was confirmed by the different chemical shift of proton 9-H in the 800 MHz ^{1}H-NMR since this proton is shielded differently depending on whether it is in proximity to either N or O in the adjacent oxazole ring. We further grew crystals of SKA-120 and SKA-121 and had them subjected to X-ray analysis, which allowed us to "see" the exact position of the N and O in the two compounds (Fig. 3). The crystal structures show two very different hydrogen bonding networks. Although SKA-120 exists as a dimer, SKA-121 has a hydrogen bonding motif that leads to a tetramer forming ribbon structures (Supplemental Fig. 1).

In summary, this SAR study demonstrated that it is possible to generate $K_{Ca}3.1$-selective activators using the naphthothiazole and the isosteric naphthooxazole scaffolds. In both cases, the presence of the 2-amino group was absolutely required for activity on both $K_{Ca}2.3$ and $K_{Ca}3.1$ channels. It was further necessary for the annulated three-ring system to be fully aromatic. Replacement of the terminal or the internal ring system with aliphatic rings reduced activity on both channels. The key position able to confer both high potency and selectivity for $K_{Ca}3.1$ seems to be the 5-position, which proved to have a very "tight" SAR. Whereas the large, lipophilic, and relatively "soft" chloride endowed the compounds with potency on both $K_{Ca}2.3$ and $K_{Ca}3.1$ (SKA-72), only CH_3 in this position produced selectivity for KCa3.1 on both the naphthothiazole (SKA-111) and the isosteric naphthooxazole (SKA-121) system.

SKA-111 and SKA-121 Are Selective KCa3.1 Activators. To fully evaluate the selectivity of the naphthothiazole SKA-111 and the naphthooxazole SKA-121, we determined seven-point concentration-response curves on $K_{Ca}2.1$, $K_{Ca}2.2$, $K_{Ca}2.3$ and $K_{Ca}3.1$ with 250 nM free Ca^{2+} in the internal solution (Fig. 4). SKA-111 and SKA-121 displayed nearly identical EC_{50} values on $K_{Ca}3.1$ (111 ± 27 nM and 109 ± 14 nM). Similar to the template SKA-31 (Sankaranarayanan et al., 2009), these effects plateaued at a roughly 30-fold maximal current increase with this intracellular Ca^{2+} concentration. Both compounds exhibited 40- to 120-fold selectivity over the three $K_{Ca}2$ channels (Fig. 4; Table 1). The Hill coefficient n_H varied between 1.6 and 3.1 in most cases, which was again similar to what had been previously reported for the template SKA-31.

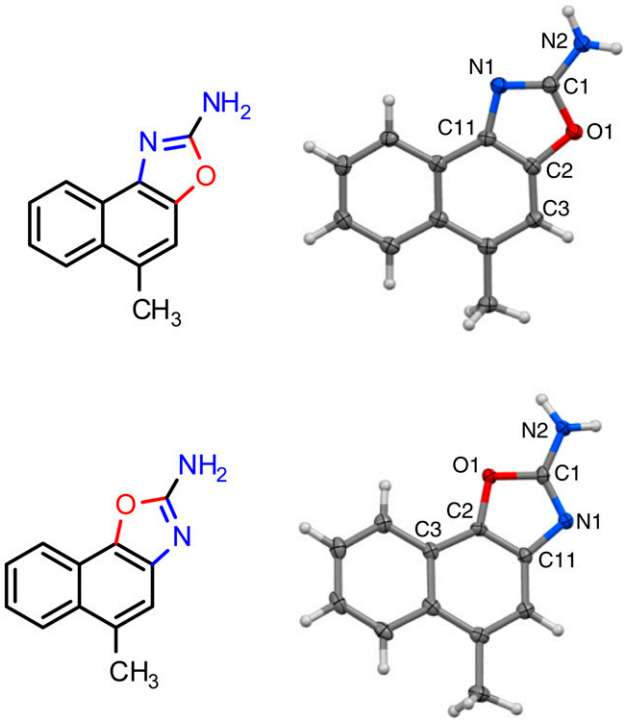

Fig. 3. X-ray crystal structures of SKA-120 (top) and SKA-121 (bottom).

We next determined the selectivity of SKA-111 and SKA-121 over more distantly related channels. At the highest reasonable and well-dissolvable test concentrations, 25 μM for SKA-111 and 50 μM for SKA-121, both compounds blocked representative members of the major K_V channel families ($K_V1.3$, $K_V2.1$, $K_V3.1$, and $K_V11.1$) by 10% to 46% (Table 1). Similarly, neuronal ($Na_V1.2$, $Na_V1.7$), skeletal muscle ($Na_V1.4$), and cardiac ($Na_V1.5$) sodium channels, as well as L-type Ca^{2+} channels ($Ca_V1.2$), were blocked by 20% to 50% by 25 μM of SKA-111 or 50 μM SKA-121. SKA-111 and SKA-121 thus displayed at least 200- to 400-fold selectivity for $K_{Ca}3.1$ over these physiologically relevant channels. Interestingly, while performing this selectivity screen, we found that N1E-115 neuroblastoma cells, a cell line established in the 1970s from a spontaneous mouse neuroblastoma tumor, are highly suitable for automated electrophysiology. The cell line produced large $Na_V1.2$ currents comparable to $Na_V1.5$ currents in a stable HEK-293 cell line (Supplemental Fig. 2).

SKA-121 is a Positive Gating Modulator of KCa3.1. Classic K_{Ca} activators like EBIO and NS309 have been shown to increase the apparent Ca^{2+}-sensitivity of K_{Ca} channels by

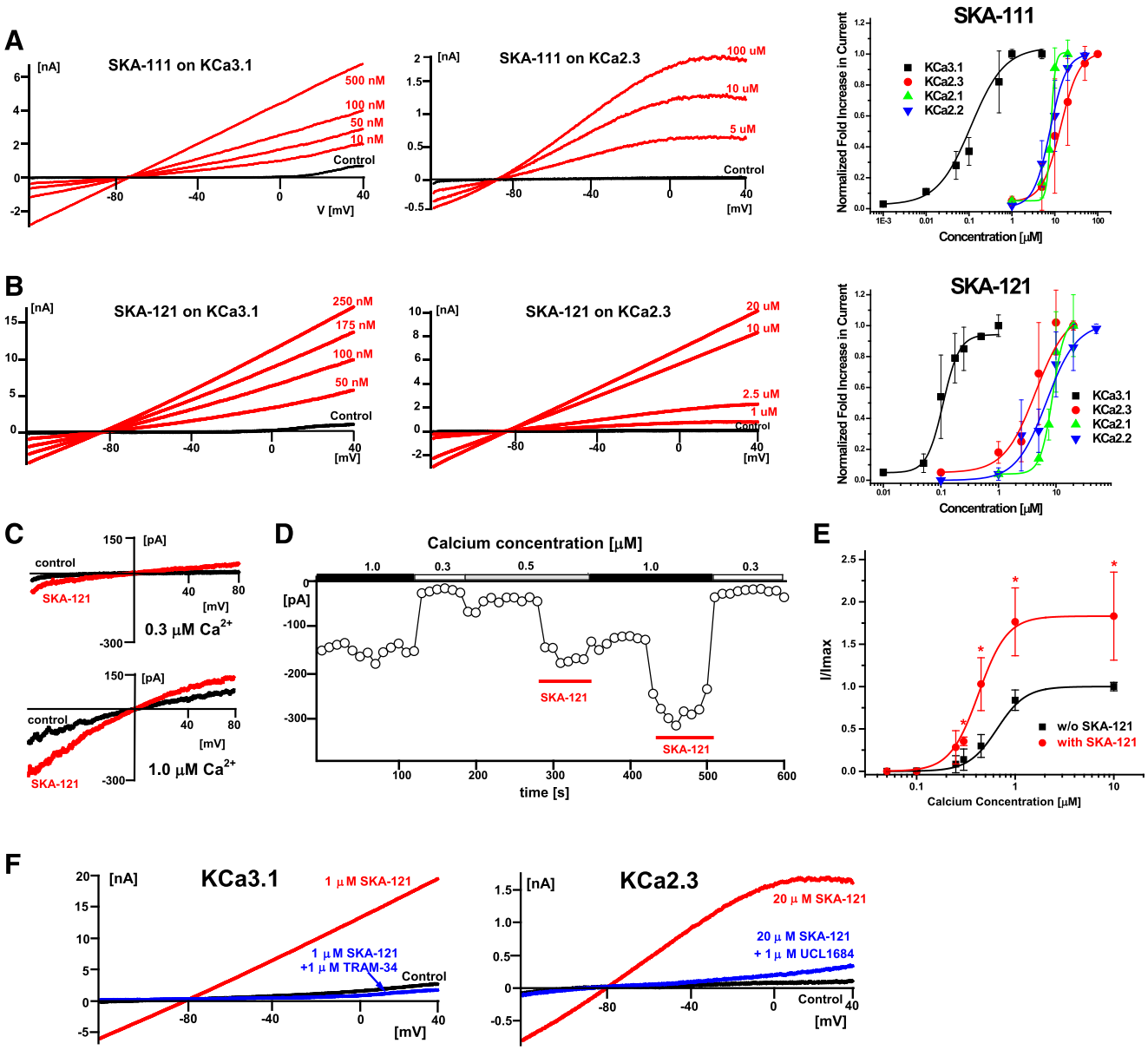

Fig. 4. SKA-111 and SKA-121 are potent and selective $K_{Ca}3.1$ activators. (A) Example traces of $K_{Ca}3.1$ and $K_{Ca}2.3$ activation by SKA-111 and concentration-response curves for $K_{Ca}3.1$ (EC_{50} 111 ± 27 nM, n_H 1.5), $K_{Ca}2.3$ (EC_{50} 13.7 ± 6.9 μM, n_H 1.9), $K_{Ca}2.1$ (EC_{50} 8.1 ± 0.4 μM, n_H 4.5), and $K_{Ca}2.2$ (EC_{50} 7.7 ± 1.9 μM, n_H 2.3). (B) Example traces of $K_{Ca}3.1$ and $K_{Ca}2.3$ activation by SKA-121 and concentration-response curves for $K_{Ca}3.1$ (EC_{50} 109 ± 14 nM, n_H 3.0), $K_{Ca}2.3$ (EC_{50} 4.4 ± 2.3 μM, n_H 1.6), $K_{Ca}2.1$ (EC_{50} 8.7 ± 1.6 μM, n_H 4.1), and $K_{Ca}2.2$ (EC_{50} 6.8 ± 2.2 μM, n_H 1.7). All data points are mean ± S.D. (C) Representative currents from inside-out patches in the presence of 0.3 μM (top) and 1 μM (bottom) Ca^{2+} before and after application of 1 μM SKA-121. (D) $K_{Ca}3.1$ current at −75 mV in an inside-out patch exposed to varying Ca^{2+} concentrations as a function of time. (Note: SKA-121 applied with 500 nM Ca^{2+} was washed out with 1 μM Ca^{2+}). (E) Ca^{2+} concentration-response curve for $K_{Ca}3.1$ activation measured from inside-out patches in the absence or presence of 1 μM SKA-121. Currents from individual patches were normalized to the effect of 10 μM Ca^{2+} in the absence of SKA-121. Data are mean ± S.D. (n = 3–5/data point; *$P < 0.05$, unpaired Student t test). An extra sum-of-squares F test (GraphPad Prism5) to compare the two curves rendered a $P < 0.0001$ for comparison of the EC_{50} values in the presence and absence of SKA-121. (F) Blockade of $K_{Ca}3.1$ and $K_{Ca}2.3$ currents activated by SKA-121 by TRAM-34 and UCL1684.

stabilizing the interaction between CaM and K_{Ca} channels (Pedarzani et al., 2001; Li et al., 2009) Since this phenomenon manifests in a leftward shift of the Ca^{2+} concentration-response curve, we performed inside-out experiments in which we varied the intracellular $[Ca^{2+}]_i$ concentration and investigated the ability of 1 μM of SKA-121 to further activate $K_{Ca}3.1$ currents at different $[Ca^{2+}]_i$ concentrations. As shown in Fig. 4C, inside-out patches pulled from h$K_{Ca}3.1$-expressing HEK-293 cells exhibited Ca^{2+}-dependent K^+ currents, reversing at 0 mV in symmetrical K^+, which could be increased further by SKA-121 at every Ca^{2+} concentration. The EC_{50} of the Ca^{2+}-concentration response curve (Fig. 4E) shifted from 650 ± 50 nM to 380 ± 95 nM in the presence of 1 μM of SKA-121, whereas the Hill coefficient was not changed by SKA-121 (n_H ~3 in both cases). Interestingly, SKA-121 not only shifted the curve to the left, but it also substantially increased the maximal achievable current at 1 and 10 μM, suggesting that the compound might be able to further increase the open probability of $K_{Ca}3.1$ at these Ca^{2+} concentrations. As expected, $K_{Ca}3.1$ currents activated by 1 μM

TABLE 1
Selectivity of SKA-111 and SKA-121 over selected ion channels
The number in parentheses indicates the number of cells used to determining the EC_{50} values or the % of current inhibition.

Channel	SKA-111 EC_{50}	SKA-121 EC_{50}
$K_{Ca}1.1$	120% of current at 25 μM (3)	115% of current at 50 μM (3)
$K_{Ca}2.1$	8.1 ± 0.4 (10)	8.7 ± 1.6 (8)
$K_{Ca}2.2$	7.7 ± 1.9 (10)	6.8 ± 1.7 (12)
$K_{Ca}2.3$	13.7 ± 6.9 (15)	4.4 ± 2.6 (18)
$K_{Ca}3.1$	0.111 ± 0.027 (24)	0.019 ± 0.014 (21)
Channel	SKA-111% current inhibition at 25 μM	SKA-121% current inhibition at 50 μM
$K_V1.3$	28.5 ± 2.3% (4)	27.5 ± 7.2% (3)
$K_V2.1$	37.3 ± 9.0% (4)	43.2 ± 12.5% (3)
$K_V3.1$	32.9 ± 1.3% (3)	46.3 ± 16.5% (4)
$K_V11.1$ (hERG)	10.1 ± 7.7% (5)	16.7 ± 9.7% (5)
$Na_V1.2$	19.5 ± 6.9% (5)	15.2 ± 12.7% (5)
$Na_V1.4$	33.4 ± 10.5% (5)	25.7 ± 1.3% (5)
$Na_V1.5$	39.9 ± 11.1% (5)	32.1 ± 11.1% (5)
$Na_V1.7$	27.5 ± 0.9% (3)	28.5 ± 1.8% (5)
$Ca_V1.2$	49.5 ± 17.0% (5)	48.9 ± 2.7% (5)

SKA-121 could be completely inhibited by 1 μM of the $K_{Ca}3.1$ pore blocker TRAM-34 (Wulff et al., 2000), whereas the $K_{Ca}2$ channel pore blocker UCL1684 (Rosa et al., 1998) had a similar effect on $K_{Ca}2.3$ currents activated by 20 μM SKA-121 (Fig. 4F).

SKA-111 and SKA-121 Increase Bradykinin-Induced Vasodilation. In addition to modulating the contractile state of the underlying vascular smooth muscle by releasing nitric oxide and prostacyclin, the vascular endothelium can induce an endothelium-derived hyperpolarization (EDH) in response to stimulation with acetylcholine or bradykinin (BK). These agonists increase $[Ca^{2+}]_i$ in the endothelium, activate $K_{Ca}3.1$ and $K_{Ca}2.3$, and induce K_{Ca}, channel-mediated hyperpolarization and arterial relaxation (Ng et al., 2008; Grgic et al., 2009; Dalsgaard et al., 2010; Edwards et al., 2010; Köhler et al., 2010; Wulff and Köhler, 2013). To demonstrate that SKA-111 and SKA-121 efficiently augment native $K_{Ca}3.1$ in PCAs and thereby potentiate BK-induced relaxation, we performed isometric myography on PCA precontracted with 0.2 μM of the vasospasmic thromboxane mimetic, U46619. SKA-111, as well as SKA-121, both at 1 μM, potentiated BK (1 μM)-induced relaxation to ≈200% and ≈300%, respectively (Fig. 5). The $K_{Ca}3.1$ blocker TRAM-34 (1 μM) prevented this potentiation and the combination of TRAM-34 and the $K_{Ca}2.3$ blocker UCL-1684 (1 μM) inhibited this potentiation slightly more effectively than TRAM-34 alone (Fig. 5).

These data from ex vivo vessel experimentation demonstrate that the $K_{Ca}3.1$-selective activators SKA-111 and SKA-121 are capable of positively modulating a physiologic response, (e.g., EDH-type vasorelaxation, in which $K_{Ca}3.1/K_{Ca}2.3$ functions have been implicated before) (Edwards et al., 2010; Wulff and Köhler, 2013).

Systemic Cardiovascular Effects of SKA-111 and SKA-121. Since we had mice implanted with telemetry leads available, we performed telemetric blood pressure measurements on wild-type and $K_{Ca}3.1^{-/-}$ mice to evaluate the cardiovascular activity and selectivity of SKA-111 and SKA-121 before performing pharmacokinetic studies. However, since we did not know the half-life when these experiments were done, we chose to start with the relatively high dose of 100 mg/kg for both compounds, reasoning that we could lower the dose in subsequent experiments. In wild-type mice, i.p. injection of 100 mg/kg SKA-111 produced a substantial drop in mean arterial blood pressure (MAP) by ~25 mmHg starting 20–30 minutes after injection (Fig. 6A, left). This decrease in MAP was significant compared with vehicle (peanut oil)-treated mice. The blood pressure drop was accompanied by a severe reduction in HR by ~400 bpm (Fig. 6A, left). To avoid fatal hypothermia or circulatory collapse, we handled these severely bradycardic mice for ~2 hours and increased RT to 34°C. As shown in Fig. 6A, these maneuvers increased MAP transiently, presumably because of a sympathetic input on total peripheral resistance, but not HR, and the low HR persisted over another 10 hours before the mice slowly recovered (Fig. 6A, left). SKA-121 at 100 mg/kg also lowered blood pressure by ~20 mmHg (Fig. 6A, right). However, this drop was more transient and lasted ~3 hours. HR was only moderately reduced (Fig. 6A, right). A lower dose of 30 mg/kg of both compounds did not produce significant alterations in MAP (Supplemental Fig. 3), whereas SKA-111 decreased HR to a minor extent (~−50 bpm for ~2 hours after injection (Supplemental Fig. 3). The vehicles, peanut oil (for SKA-111) or peanut oil/DMSO (9:1 v/v, for SKA-121), did not cause significant alterations in MAP or HR (Fig. 6A).

We next tested whether SKA-111 and SKA-121 are also efficient in lowering the higher MAP caused by systemic inhibition of nitric oxide production by L-NAME administered in the drinking water (Fig. 6B). However, for these experiments, we used a lower dose (60 mg/kg) of SKA-111 to avoid causing such a severe drop of HR as observed with 100 mg/kg. The 60 mg/kg dose produced only a minor drop in MAP and HR. In contrast, SKA-121 at 100 mg/kg produced a significant drop in MAP by ~25 mmHg over 6 hours. This drop was accompanied by a minor decrease in HR (Fig. 6B, right).

We next evaluated the $K_{Ca}3.1$ selectivity by using $KCa3.1^{-/-}$ mice and found that SKA-111 at 100 mg/kg also produced a significant drop in MAP by ~15 mmHg lasting ~16 hours in these animals (Fig. 6C, left). Similar to wild-type mice, HR decreased substantially by ~400 beats/minute over ~22 hours (Fig. 6C, *left*). Similar to the results in wild-type mice, the lower dose of 30 mg/kg also significantly reduced HR, although less dramatically and not for as long as the higher dose. MAP did not change with the 30 mg/kg dose of SKA-111 (Fig. 6C, left). In contrast to SKA-111, SKA-121 at 100 mg/kg had no significant effects on MAP and HR in the $K_{Ca}3.1^{-/-}$ mice (Fig. 6C, right).

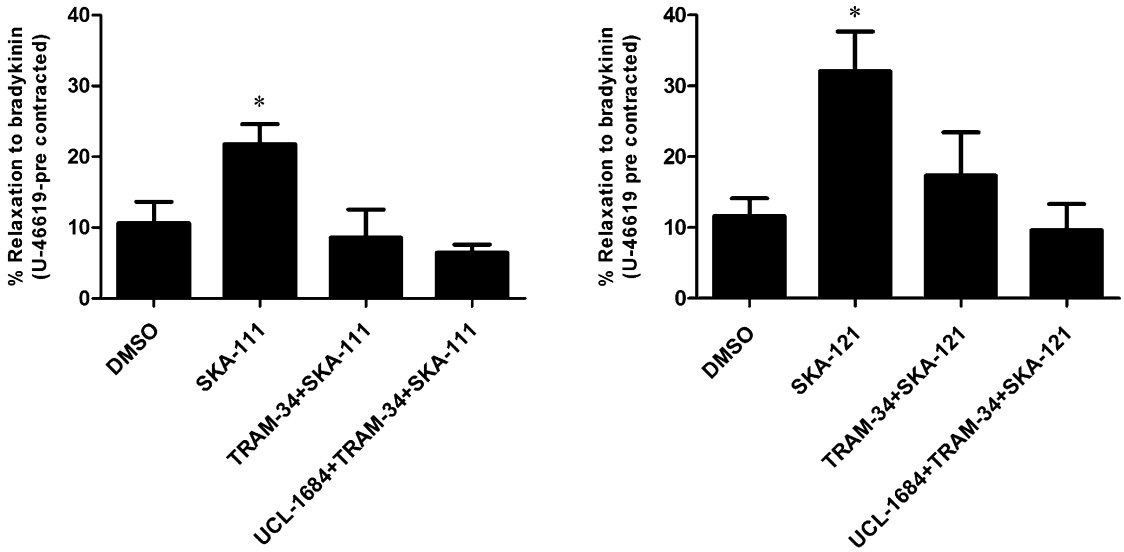

Fig. 5. Isometric myography. SKA-111 and SKA-121 (both at 1 μM) increased BK-induced EDH-type relaxation of U46619-precontracted PCA rings in the presence of blockers of NO synthesis (L-NNA) and cyclooxygenases (indomethacin). TRAM-34 (1 μM) alone and the combination of TRAM-34 and UCL-1684 (1 μM) prevented the increase of relaxation. Data are mean ± S.E.M., n = 5–22 PCA. *$P < 0.05$, unpaired Student's t test.

Taken together, these telemetry experiments showed that both compounds exhibited cardiovascular activity in vivo as they substantially reduce basal blood pressure and the higher blood pressure caused by NO deficiency. Moreover, SKA-121 produced this blood pressure–lowering action in a $K_{Ca}3.1$-dependent manner as suggested by lack of MAP-lowering effects in $K_{Ca}3.1^{-/-}$ mice. In contrast, SKA-111 lowered MAP and induced a strong HR reduction independently of $K_{Ca}3.1$.

Pharmacokinetics of SKA-111 and SKA-121. To help us better interpret the results of the telemetry experiments, we established ultraperformance liquid chromatography (UPLC)/mass spectrometry (MS) assays for SKA-111 and SKA-121 based on an high-performance LC/MS assay we had previously published for SKA-31 (Sankaranarayanan et al., 2009) and performed some basic pharmacokinetic studies with both compounds in mice. After i.v. injection at 10 mg/kg into the tail vein, total SKA-111 plasma concentrations fell biexponentially, reflecting a two-compartment model with very rapid distribution from blood into tissue (~2 minutes), followed by elimination with a half-life of 4.7 ± 0.6 hours (Fig. 7A). SKA-121, in contrast, had a much shorter half-life (~20 minutes), and plasma decay was extremely rapid (21.3 ± 2.4 μM at 5 minutes; 483 ± 231 nM at 1 hour and 53 ± 44 nM at 4 hours). Since SKA-121 is relatively well soluble (log$P$ = 1.79) and could potentially be added to drinking water in animal experiments, we also administered it orally and found that it had an oral availability of roughly 25% (Fig. 7B). But again, plasma levels dropped rapidly from 1.1 ± 0.1 μM at 1 hour after oral administration to 27 ± 5 nM at 8 hours. Plasma protein binding was 59% ± 2% (n = 3) for SKA-111 and 81% ± 4% (n = 2) for SKA-121. Since we had also removed brains from the mice when obtaining blood samples by cardiac puncture (which had been done at every third blood collection), we further determined total brain concentrations at various time points and obtained averaged brain/plasma ratios for both compounds from times when the compounds were detectable in both plasma and brain. SKA-111 proved highly brain penetrant with a brain-to-plasma ratio of 9.3 ± 5.3. SKA-121 was less brain penetrant but still very effectively partitioned into the brain with a brain/plasma ratio of 3.3 ± 2.9 (Fig. 7C).

Taken together, these results explain why SKA-111 had a much more prolonged blood pressure–lowering effect in the telemetry experiments in Fig. 6 than did SKA-121. The fact that SKA-111 is highly brain penetrant and probably achieved total brain concentrations in the range of 10–30 μM for hours after i.p. administration at 100 mg/kg also provides an explanation for why this $K_{Ca}3.1$ selective compound "lost" its selectivity in vivo and reduced blood pressure and heart rate, side effects that are presumably mediated by $K_{Ca}2$ channel activation in the central nervous system as well as $K_{Ca}2$ channel activation in resistance arteries and the heart (Radtke et al., 2013) and also occurred in $K_{Ca}3.1^{-/-}$ mice (Fig. 6C, left). In keeping with its shorter half-life of only 20 minutes and its lower brain penetration, SKA-121 induced a significant but less prolonged drop in MAP in the telemetry experiments when administered i.p. at 100 mg/kg (Fig. 6A *right*) and exhibited $K_{Ca}3.1$ selectivity in vivo as suggested by the lack of MAP-lowering effects in $K_{Ca}3.1^{-/-}$ mice and its insignificant effect on heart rate in wild-type mice.

Discussion

We here used our previously described mixed $K_{Ca}2/3$ channel activator SKA-31 (Sankaranarayanan et al., 2009) as a template for the design of two selective $K_{Ca}3.1$ activators. Both molecules, SKA-111 and SKA-121, activate $K_{Ca}3.1$ with EC_{50}s of ~110 nM and display 40- to 120-fold selectivity for $K_{Ca}3.1$ over the three $K_{Ca}2$ channels ($K_{Ca}2.1$, $K_{Ca}2.2$, and $K_{Ca}2.3$). These compounds constitute the first pharmacological or chemical biology tools that can be used to selectively activate $K_{Ca}3.1$ channels in tissue preparations or in vivo without performing

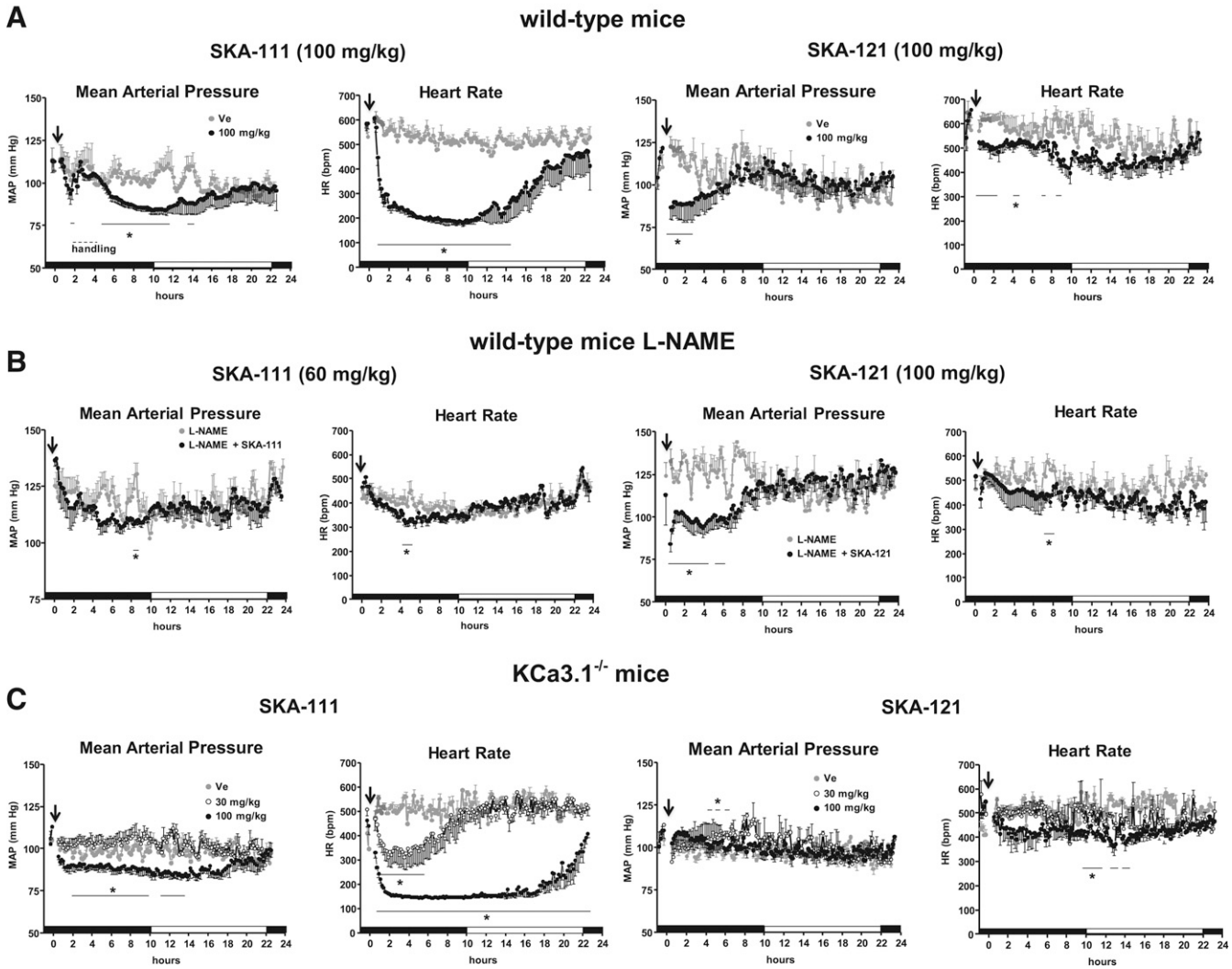

Fig. 6. Blood pressure telemetry. (A) Injections (i.p.) of SKA-111 (panels on left) and SKA-121 (panels on right) reduced MAP in wild-type mice. SKA-111 (on left), but not SKA-121 (on right), severely reduced HR. As indicated by the dashed line (right panel), SKA-111–treated animals were initially handled and warmed to avoid fatal hypothermia during strong bradycardia. Ve, vehicle control. Black and white marked intervals of *x*-axis indicate dark and light periods. (B) SKA-121 (on right) but, to a lesser extent, SKA-111 (on left), reduced blood pressure in L-NAME–treated moderately hypertensive mice. HR remained virtually stable. (C) Cardiovascular actions of SKA-111 and SKA-121 in KCa3.1$^{-/-}$ mice. At 100 mg/kg, SKA-111 but not SKA-121 reduced MAP and HR. SKA-111 also reduced HR at 30 mg/kg. Data points are means ± S.E.M.; n = 3 or 4 experiments/strain and compound. Lines indicate time periods when pressures or HRs were significantly different from Ve. *$P < 0.05$, unpaired Student's t test.

additional manipulations such as genetically knocking out or pharmacologically blocking $K_{Ca}2$ channels.

According to the definition of *positive-gating modulation*, compounds like EBIO and NS309 act by shifting the Ca^{2+}-activation curve of $K_{Ca}2/3$ channels to the left, meaning that the determined EC_{50} values for Ca^{2+}-dependent channel activation calculated from Ca^{2+}-concentration response curves decrease in the presence of the modulator molecule. For NS309, studies using CaM mutants making unstable association with the CaMB of $K_{Ca}2.2$ have shown that NS309 increases the apparent Ca^{2+}-sensitivity of K_{Ca} channels by stabilizing the interaction between CaM and the CaMBD of the K_{Ca} channels (Pedarzani et al., 2001; Li et al., 2009). More recently, Zhang et al. (2012) crystallized CaM bound to the CaMBD of $K_{Ca}2.2$ and afterward soaked EBIO into the crystal. In a subsequent study, the same group obtained a cocrystal of the CaM/CaMBD with NS309 (Zhang et al., 2013). Both molecules reside in a pocket formed at the interface between CaM/CaMBD. Interestingly, on NS309 binding, an intrinsically disordered stretch of 16 amino acids that connects S6 to the CaMBD and was not visible in the EBIO/CaM/CaMBD crystal becomes visible, suggesting that it undergoes a transition to a well-defined structure. Other manipulations of this S6-CaMBD linker region, such as cross-linking a residue in the region to a residue in the CaMBD, also increase channel activity and apparent Ca^{2+} sensitivity, demonstrating that this linker region plays a crucial role in coupling Ca^{2+} binding to CaM to the mechanical opening of K_{Ca} channels (Zhang et al., 2013). By changing the confirmation of this linker region, NS309 is thus "truly" a gating modulator and we assume that SKA-111 and SKA-121 are exerting their effects in a similar manner. We have not yet mapped their binding sites, but we have also observed that mutations of the analogous residues in the CaMBD of $K_{Ca}2.3$, which had been reported to increase or decrease the potency of EBIO for activating $K_{Ca}2.2$ (Zhang et al., 2012), also significantly altered the potency of SKA-31 (Brown et al., 2014) suggesting that, similar to EBIO and NS309, benzothiazole-type $K_{Ca}2/3$ activators bind at the

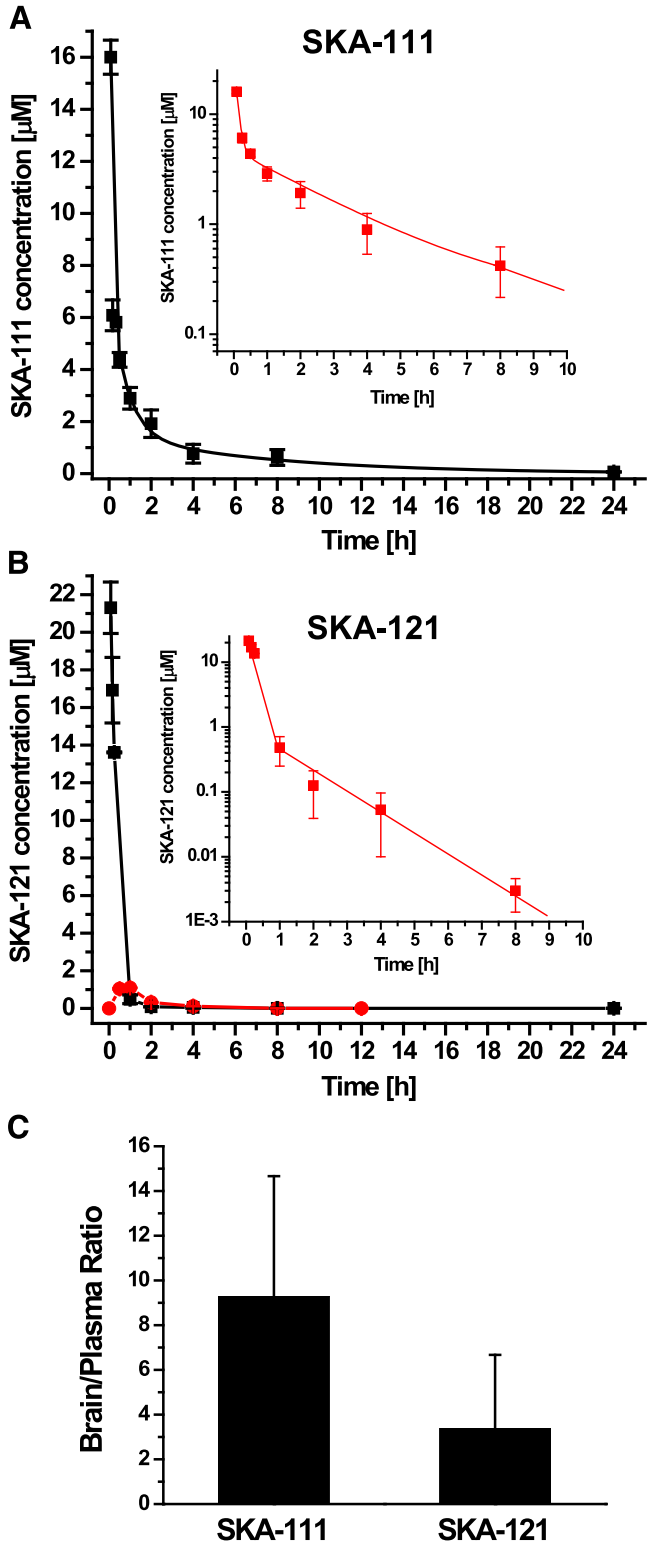

Fig. 7. Pharmacokinetics of SKA-111 and SKA-121. (A) Total SKA-111 plasma concentration (mean ± S.D.) after i.v. administration of 10 mg/kg to mice (n = 2 to 3 per time point; $t_{1/2}$ Distribution ~2 minutes; $t_{1/2}$ elimination = 4.7 ± 0.6 hours). Inset: The first 10 hours on a log scale. (B) Total SKA-121 plasma concentrations (mean ± S.D.) after i.v. (black) and oral (red) application of 10 mg/kg to mice (n = 3/time point; $t_{1/2}$ ~20 minutes; oral availability ~25%). Inset: The first 10 hours after i.v. administration on a log scale. (C) Brain-to-plasma concentration ratios for SKA-111 and SKA-121 determined from multiple paired brain and plasma samples obtained during the experiments shown in (A) and (B) (n = 8 for SKA-111 and n = 5 for SKA-121).

interface between CaM/CaMBD. This interface pocket is relatively "tight," and the CaMBD shows a number of sequence differences between the four K_{Ca} channels, making it appear plausible that a "minor" structural change such as adding a $-CH_3$ in 5-position of SKA-31 can increase selectivity for $K_{Ca}3.1$ from 10-fold to 100-fold in SKA-111. This hypothesis that SKA-31, SKA-111, and SKA-121 are binding to the same site in the CaM/CaMBD interface as NS309 agrees well with the relatively steep structure-activity-relationship we observed in our study. For the napthobenzothiazole and the isosteric naphthooxazole system, potency and selectivity for $K_{Ca}3.1$ over $K_{Ca}2$ channels were very sensitive to the exact position and electronic nature of substituents (e.g., SKA-106 and SKA-109 in Fig. 2). Another interesting observation in this context is that SKA-121 not only shifted the concentration-response curve for Ca^{2+}-dependent $K_{Ca}3.1$ activation to the left but also increased the maximal achievable current at 1 and 10 μM in inside-out patches (Fig. 4). Since none of the benzothiazole-type $K_{Ca}2/3$ activators, including SKA-31, SKA-111, SKA-121, and their many derivatives, had ever increased $K_{Ca}3.1$ or $K_{Ca}2$ currents in our hands at Ca^{2+} concentrations lower than 100 nM or in the absence of Ca^{2+} with KF-based pipette solutions, we do not ascribe this effect to a direct channel opening component in their mechanism of action, like that reported for GW542573X and (-)-CM-TMPF for $K_{Ca}2.1$ (Hougaard et al., 2009, 2012). Unlike SKA-121, which we think is binding at the CaM/CaMBD interface, (-)CM-TMPF has been found to interact with positions deep within the inner pore vestibule (Hougaard et al., 2012) close to the selectivity filter, where the gate of $K_{Ca}2/3$ channels seems to be located (Bruening-Wright et al., 2002, 2007; Garneau et al., 2009; Klein et al., 2007). It therefore seems reasonable to attribute the Ca^{2+}-independent $K_{Ca}2.1$ channel activation by (-)-CM-TMPF to a directly opening effect on the gate and use this explanation to account for the fact that (-)-CM-TMPF increases $K_{Ca}2.1$ currents to roughly 40% of their maximal activity at Ca^{2+} concentrations between 10 and 100 nM and then levels off in its opening/activating activity at higher Ca^{2+} concentrations (Hougaard et al., 2012). Since this is clearly not the case for SKA-121, which in contrast further increases maximal channel activity at 1 and 10 μM of Ca^{2+}, we believe that SKA-121 is a "classic" positive gating modulator, which requires the presence of Ca^{2+} to enhance K_{Ca} channel activity but by stabilizing the interaction between CaM and the CaMBD of $K_{Ca}3.1$ is also able to further increase the Ca^{2+}-dependent open channel probability P_o(max) value of $K_{Ca}3.1$. Unlike $K_{Ca}2$ channels, which are assumed to be fully open at saturating $[Ca_{2+}]_i$ concentrations, $K_{Ca}3.1$ channels have been reported to have a relatively low Ca^{2+}-dependent P_o(max), which can be increased significantly by the addition of 1.6 mM MgATP (Gerlach et al., 2001; Jones et al., 2007) or by mutations of residues in S5 (Garneau et al., 2014). We here left out ATP from the internal solutions for inside-out and whole-cell recordings on purpose to not confuse the analysis by having too many variables.

Since $K_{Ca}3.1$ is involved in EDH-mediated vasodilator responses and has been accordingly suggested as a potential new antihypertensive pharmacological target (Grgic et al., 2009; Dalsgaard et al., 2010; Edwards et al., 2010; Köhler et al., 2010), we tested the effect of both of our new $K_{Ca}3.1$ selective activators, SKA-111 and SKA-121, on BK-induced EDH responses in vitro on porcine coronary arteries and on blood

pressure in mice. Both compounds potentiated BK effects in vitro and robustly lower blood pressure in mice in vivo. However, as these experiments and subsequently performed pharmacokinetic studies showed, both compounds do not have ideal properties for development into a potential antihypertensive drug candidate. SKA-111 is so highly brain penetrant that it achieves roughly ~10-fold higher concentrations in the central nervous system and may thus cause complex neurologic side effects by activating neuronal $K_{Ca}2$ channels (Adelman et al., 2012). Moreover, SKA-111 induces the same severe bradycardia that had also been a problem when the unselective SKA-31 was dosed at 100 mg/kg in connexin 40–deficient mice (Radtke et al., 2013). This bradycardia is especially impressive in that it occurs also in KCa3.1$^{-/-}$ mice (Fig. 6) and is probably due to direct effects on $K_{Ca}2$ channels in cardiac pacemaker tissue (Radtke et al., 2013), as well as to a possible a central decrease in sympathetic drive through activation of neuronal $K_{Ca}2$ channels. SKA-121 is less brain penetrant and largely maintains its $K_{Ca}3.1$ selectivity in vivo. It lowers blood pressure in both normotensive and hypertensive mice without significantly reducing heart rate or affecting blood pressure in $K_{Ca}3.1^{-/-}$ mice. However, a problem with SKA-121 is the extremely short 20-minute half-life in mice, which would necessitate continuous infusion for blood pressure studies, a depot, or very frequently repeated drug applications. In this respect, it should, of course, be explored if SKA-121 possibly has a longer half-life in larger animals such as dogs, pigs, or primates.

In summary, with SKA-111 and SKA-121, we have identified two $K_{Ca}3.1$-selective positive gating modulators that constitute novel pharmacological tools for further dissecting the role of $K_{Ca}3.1$ in EDH and systemic blood pressure and that could help determine whether $K_{Ca}3.1$ activators could eventually be developed into a new class of endothelial targeted antihypertensive agents. Other potential indications for $K_{Ca}3.1$ activators could be intrasurgical hypertension, acute vasospasm, or preservation of endothelial function in large vascular organs such as the heart or kidneys or in vessel grafts during storage and transplantation. $K_{Ca}3.1$ activators have also long been suggested for enhancing fluid secretion in cystic fibrosis (Singh et al., 2001). Although SKA-111 and SKA-121 are not ideal candidate molecules, they could serve as templates for the design of derivatives with pharmacokinetic properties more suitable for further development and innovation.

Acknowledgments

The authors thank Dr. Eduardo Romanos-Alfonos and Susana Murillo-Pola of the Unit of Functional Evaluations of the IACS for excellent technical support (telemetry).

Authorship Contributions

Participated in research design: Coleman, Brown, Valero, Oliván-Viguera, Köhler, Wulff.

Conducted experiments: Coleman, Brown, Singh, Valero, Oliván-Viguera, Olmstead.

Performed data analysis: Coleman, Brown, Heike Wulff.

Wrote or contributed to the writing of the manuscript: Coleman, Brown, Singh, Oliván-Viguera, Köhler, Wulff.

References

Adelman JP, Maylie J, and Sah P (2012) Small-conductance Ca^{2+}-activated K^+ channels: form and function. *Annu Rev Physiol* **74**:245–269.

Balut CM, Hamilton KL, and Devor DC (2012) Trafficking of intermediate (KCa3.1) and small (KCa2.x) conductance, $Ca^{(2+)}$-activated $K^{(+)}$ channels: a novel target for medicinal chemistry efforts? *ChemMedChem* **7**:1741–1755.

Blank T, Nijholt I, Kye MJ, Radulovic J, and Spiess J (2003) Small-conductance, Ca^{2+}-activated K^+ channel SK3 generates age-related memory and LTP deficits. *Nat Neurosci* **6**:911–912.

Brähler S, Kaistha A, Schmidt VJ, Wölfle SE, Busch C, Kaistha BP, Kacik M, Hasenau AL, Grgic I, and Si H et al. (2009) Genetic deficit of SK3 and IK1 channels disrupts the endothelium-derived hyperpolarizing factor vasodilator pathway and causes hypertension. *Circulation* **119**:2323–2332.

Brown BM, Coleman N, Oliván-Viguera A, Köhler R, Wulff H (2014) Positive KCa channel gating modulators with selectivity for KCa3.1. *FASEB J* 28:1057.6.

Bruening-Wright A, Lee WS, Adelman JP, and Maylie J (2007) Evidence for a deep pore activation gate in small conductance Ca^{2+}-activated K^+ channels. *J Gen Physiol* **130**:601–610.

Bruening-Wright A, Schumacher MA, Adelman JP, and Maylie J (2002) Localization of the activation gate for small conductance Ca^{2+}-activated K^+ channels. *J Neurosci* **22**:6499–6506.

Dalsgaard T, Kroigaard C, and Simonsen U (2010) Calcium-activated potassium channels - a therapeutic target for modulating nitric oxide in cardiovascular disease? *Expert Opin Ther Targets* **14**:825–837.

Damkjaer M, Nielsen G, Bodendiek S, Staehr M, Gramsbergen JB, de Wit C, Jensen BL, Simonsen U, Bie P, and Wulff H et al. (2012) Pharmacological activation of KCa3.1/KCa2.3 channels produces endothelial hyperpolarization and lowers blood pressure in conscious dogs. *Br J Pharmacol* **165**:223–234.

Debono MW, Le Guern J, Canton T, Doble A, and Pradier L (1993) Inhibition by riluzole of electrophysiological responses mediated by rat kainate and NMDA receptors expressed in Xenopus oocytes. *Eur J Pharmacol* **235**:283–289.

Devor DC, Singh AK, Frizzell RA, and Bridges RJ (1996) Modulation of Cl^- secretion by benzimidazolones. I. Direct activation of a $Ca^{(2+)}$-dependent K^+ channel. *Am J Physiol* **271**:L775–L784.

Duprat F, Lesage F, Patel AJ, Fink M, Romey G, and Lazdunski M (2000) The neuroprotective agent riluzole activates the two P domain $K^{(+)}$ channels TREK-1 and TRAAK. *Mol Pharmacol* **57**:906–912.

Edwards G, Félétou M, and Weston AH (2010) Endothelium-derived hyperpolarising factors and associated pathways: a synopsis. *Pflugers Arch* **459**: 863–879.

Fanger CM, Ghanshani S, Logsdon NJ, Rauer H, Kalman K, Zhou J, Beckingham K, Chandy KG, Cahalan MD, and Aiyar J (1999) Calmodulin mediates calcium-dependent activation of the intermediate conductance KCa channel, IKCa1. *J Biol Chem* **274**:5746–5754.

Garneau L, Klein H, Banderali U, Longpré-Lauzon A, Parent L, and Sauvé R (2009) Hydrophobic interactions as key determinants to the KCa3.1 channel closed configuration: an analysis of KCa3.1 mutants constitutively active in zero Ca^{2+}. *J Biol Chem* **284**:389–403.

Garneau L, Klein H, Lavoie MF, Brochiero E, Parent L, and Sauvé R (2014) Aromatic-aromatic interactions between residues in KCa3.1 pore helix and S5 transmembrane segment control the channel gating process. *J Gen Physiol* **143**: 289–307.

Gerlach AC, Syme CA, Giltinan L, Adelman JP, and Devor DC (2001) ATP-dependent activation of the intermediate conductance, Ca^{2+}-activated K^+ channel, hIK1, is conferred by a C-terminal domain. *J Biol Chem* **276**:10963–10970.

Göblyös A, Santiago SN, Pietra D, Mulder-Krieger T, von Frijtag Drabbe Künzel J, Brussee J, and Ijzerman AP (2005) Synthesis and biological evaluation of 2-aminothiazoles and their amide derivatives on human adenosine receptors. Lack of effect of 2-aminothiazoles as allosteric enhancers. *Bioorg Med Chem* **13**: 2079–2087.

Grgic I, Kaistha BP, Hoyer J, and Köhler R (2009) Endothelial Ca+-activated K+ channels in normal and impaired EDHF-dilator responses: relevance to cardiovascular pathologies and drug discovery. *Br J Pharmacol* **157**:509–526.

Grissmer S, Nguyen AN, Aiyar J, Hanson DC, Mather RJ, Gutman GA, Karmilowicz MJ, Auperin DD, and Chandy KG (1994) Pharmacological characterization of five cloned voltage-gated K^+ channels, types Kv1.1, 1.2, 1.3, 1.5, and 3.1, stably expressed in mammalian cell lines. *Mol Pharmacol* **45**:1227–1234.

Grunnet M, Jespersen T, Angelo K, Frøkjaer-Jensen C, Klaerke DA, Olesen SP, and Jensen BS (2001) Pharmacological modulation of SK3 channels. *Neuropharmacology* **40**: 879–887.

Hougaard C, Eriksen BL, Jørgensen S, Johansen TH, Dyhring T, Madsen LS, Strøbaek D, and Christophersen P (2007) Selective positive modulation of the SK3 and SK2 subtypes of small conductance Ca^{2+}-activated K^+ channels. *Br J Pharmacol* **151**:655–665.

Hougaard C, Hammami S, Eriksen BL, Sørensen US, Jensen ML, Strøbæk D, and Christophersen P (2012) Evidence for a common pharmacological interaction site on K(Ca)2 channels providing both selective activation and selective inhibition of the human K(Ca)2.1 subtype. *Mol Pharmacol* **81**:210–219.

Hougaard C, Jensen ML, Dale TJ, Miller DD, Davies DJ, Eriksen BL, Strøbaek D, Trezise DJ, and Christophersen P (2009) Selective activation of the SK1 subtype of human small-conductance Ca^{2+}-activated K^+ channels by 4-(2-methoxyphenylcarbamoyloxymethyl)-piperidine-1-carboxylic acid tert-butyl ester (GW542573X) is dependent on serine 293 in the S5 segment. *Mol Pharmacol* **76**:569–578.

Jenkins DP, Yu W, Brown BM, Løjkner LD, and Wulff H (2013) Development of a QPatch automated electrophysiology assay for identifying KCa3.1 inhibitors and activators. *Assay Drug Dev Technol* **11**:551–560.

Joiner WJ, Wang LY, Tang MD, and Kaczmarek LK (1997) hSK4, a member of a novel subfamily of calcium-activated potassium channels. *Proc Natl Acad Sci USA* **94**:11013–11018.

Jones HM, Bailey MA, Baty CJ, Macgregor GG, Syme CA, Hamilton KL, and Devor DC (2007) An NH_2-terminal multi-basic RKR motif is required for the ATP-dependent regulation of hIK1. *Channels (Austin)* **1**:80–91.

Jordan AD, Luo C, and Reitz AB (2003) Efficient conversion of substituted aryl thioureas to 2-aminobenzothiazoles using benzyltrimethylammonium tribromide. *J Org Chem* **68**:8693–8696.

Kasumu AW, Hougaard C, Rode F, Jacobsen TA, Sabatier JM, Eriksen BL, Strøbæk D, Liang X, Egorova P, and Vorontsova D et al. (2012) Selective positive modulator

of calcium-activated potassium channels exerts beneficial effects in a mouse model of spinocerebellar ataxia type 2. *Chem Biol* **19**:1340–1353.
Klein H, Garneau L, Banderali U, Simoes M, Parent L, and Sauvé R (2007) Structural determinants of the closed KCa3.1 channel pore in relation to channel gating: results from a substituted cysteine accessibility analysis. *J Gen Physiol* **129**:299–315.
Köhler M, Hirschberg B, Bond CT, Kinzie JM, Marrion NV, Maylie J, and Adelman JP (1996) Small-conductance, calcium-activated potassium channels from mammalian brain. *Science* **273**:1709–1714.
Köhler R (2012) Cardiovascular alterations in KCa3.1/KCa2.3-deficient mice and after acute treatment with KCa3.1/KCa2.3 activators. *EDHF 2012: 10th Anniversary Meeting* June 27th - 30th, 2012; Feletou M, Vanhoutte PM (eds) vol. 49, pp 1–54 Vaux-de-Cernay, France.
Köhler R, Kaistha BP, and Wulff H (2010) Vascular KCa-channels as therapeutic targets in hypertension and restenosis disease. *Expert Opin Ther Targets* **14**:143–155.
Li W, Halling DB, Hall AW, and Aldrich RW (2009) EF hands at the N-lobe of calmodulin are required for both SK channel gating and stable SK-calmodulin interaction. *J Gen Physiol* **134**:281–293.
Ng KF, Leung SW, Man RY, and Vanhoutte PM (2008) Endothelium-derived hyperpolarizing factor mediated relaxations in pig coronary arteries do not involve Gi/o proteins. *Acta Pharmacol Sin* **29**:1419–1424.
Pedarzani P, Mosbacher J, Rivard A, Cingolani LA, Oliver D, Stocker M, Adelman JP, and Fakler B (2001) Control of electrical activity in central neurons by modulating the gating of small conductance Ca^{2+}-activated K^+ channels. *J Biol Chem* **276**:9762–9769.
Radtke J, Schmidt K, Wulff H, Köhler R, and de Wit C (2013) Activation of KCa3.1 by SKA-31 induces arteriolar dilatation and lowers blood pressure in normo- and hypertensive connexin40-deficient mice. *Br J Pharmacol* **170**:293–303.
Rosa JC, Galanakis D, Ganellin CR, Dunn PM, and Jenkinson DH (1998) Bis-quinolinium cyclophanes: 6,10-diaza-3(1,3),8(1,4)-dibenzena-1,5(1,4)- diquinolinacyclodecaphane (UCL 1684), the first nanomolar, non-peptidic blocker of the apamin-sensitive $Ca^{(2+)}$-activated K^+ channel. *J Med Chem* **41**:2–5.
Sankaranarayanan A, Raman G, Busch C, Schultz T, Zimin PI, Hoyer J, Köhler R, and Wulff H (2009) Naphtho[1,2-*d*]thiazol-2-ylamine (SKA-31), a new activator of KCa2 and KCa3.1 potassium channels, potentiates the endothelium-derived hyperpolarizing factor response and lowers blood pressure. *Mol Pharmacol* **75**:281–295.
Schmitz A, Sankaranarayanan A, Azam P, Schmidt-Lassen K, Homerick D, Hänsel W, and Wulff H (2005) Design of PAP-1, a selective small molecule Kv1.3 blocker, for the suppression of effector memory T cells in autoimmune diseases. *Mol Pharmacol* **68**:1254–1270.
Schuart J and Müller HK (1973) [2-Aminooxazoles and 2-iminooxazolines. 1: reaction of racemic alpha-methylaminopropiophenone using cyanobromide]. *Pharmazie* **28**:438–439.
Sheldrick GM (2008) A short history of SHELX. *Acta Crystallogr A* **64**:112–122.
Singh S, Syme CA, Singh AK, Devor DC, and Bridges RJ (2001) Benzimidazolone activators of chloride secretion: potential therapeutics for cystic fibrosis and chronic obstructive pulmonary disease. *J Pharmacol Exp Ther* **296**:600–611.
Strøbaek D, Teuber L, Jørgensen TD, Ahring PK, Kjaer K, Hansen RS, Olesen SP, Christophersen P, and Skaaning-Jensen B (2004) Activation of human IK and SK Ca^{2+} -activated K^+ channels by NS309 (6,7-dichloro-1*H*-indole-2,3-dione 3-oxime). *Biochim Biophys Acta* **1665**:1–5.
Wei AD, Gutman GA, Aldrich R, Chandy KG, Grissmer S, and Wulff H (2005) International Union of Pharmacology. LII. Nomenclature and molecular relationships of calcium-activated potassium channels. *Pharmacol Rev* **57**:463–472.
Wulff H and Köhler R (2013) Endothelial small-conductance and intermediate-conductance KCa channels: an update on their pharmacology and usefulness as cardiovascular targets. *J Cardiovasc Pharmacol* **61**:102–112.
Wulff H, Miller MJ, Hansel W, Grissmer S, Cahalan MD, and Chandy KG (2000) Design of a potent and selective inhibitor of the intermediate-conductance Ca^{2+} -activated K^+ channel, IKCa1: a potential immunosuppressant. *Proc Natl Acad Sci USA* **97**:8151–8156.
Wulff H and Zhorov BS (2008) K^+ channel modulators for the treatment of neurological disorders and autoimmune diseases. *Chem Rev* **108**:1744–1773.
Xia XM, Fakler B, Rivard A, Wayman G, Johnson-Pais T, Keen JE, Ishii T, Hirschberg B, Bond CT, and Lutsenko S et al. (1998) Mechanism of calcium gating in small-conductance calcium-activated potassium channels. *Nature* **395**:503–507.
Zhang M, Pascal JM, Schumann M, Armen RS, and Zhang JF (2012) Identification of the functional binding pocket for compounds targeting small-conductance Ca^{2+}-activated potassium channels. *Nat Commun* **3**:1021.
Zhang M, Pascal JM, and Zhang JF (2013) Unstructured to structured transition of an intrinsically disordered protein peptide in coupling Ca^{2+}-sensing and SK channel activation. *Proc Natl Acad Sci USA* **110**:4828–4833.

Address correspondence to: Heike Wulff, Department of Pharmacology, Genome and Biomedical Sciences Facility, Room 3502, 451 Health Sciences Drive, University of California, Davis, Davis, CA 95616. E-mail: hwulff@ucdavis.edu